Published Ahead of Print on April 19, 2019, as doi:10.3324/haematol.2018.206631.
Copyright 2019 Ferrata Storti Foundation.

haematologica
Journal of The Ferrata Storti Foundation

Non-genotoxic MDM2 inhibition selectively induces pro-apoptotic p53 gene signature in chronic lymphocytic leukemia cells

by Carmela Ciardullo, Erhan Aptullahoglu, Laura Woodhouse, Wei-Yu Lin, Jonathan P. Wallis, Helen Marr, Scott Marshall, Nick Bown, Elaine Willmore, and John Lunec

Haematologica 2019 [Epub ahead of print]

Citation: Carmela Ciardullo, Erhan Aptullahoglu, Laura Woodhouse, Wei-Yu Lin, Jonathan P. Wallis, Helen Marr, Scott Marshall, Nick Bown, Elaine Willmore, and John Lunec. Non-genotoxic MDM2 inhibition selectively induces pro-apoptotic p53 gene signature in chronic lymphocytic leukemia cells. Haematologica. 2019; 104:xxx
doi:10.3324/haematol.2018.206631

Publisher's Disclaimer.
E-publishing ahead of print is increasingly important for the rapid dissemination of science. Haematologica is, therefore, E-publishing PDF files of an early version of manuscripts that have completed a regular peer review and have been accepted for publication. E-publishing of this PDF file has been approved by the authors. After having E-published Ahead of Print, manuscripts will then undergo technical and English editing, typesetting, proof correction and be presented for the authors' final approval; the final version of the manuscript will then appear in print on a regular issue of the journal. All legal disclaimers that apply to the journal also pertain to this production process.

Non-genotoxic MDM2 inhibition selectively induces pro-apoptotic p53 gene signature in chronic lymphocytic leukemia cells

Carmela Ciardullo[1], Erhan Aptullahoglu[1], Laura Woodhouse[2], Wei-Yu Lin[2], Jonathan P Wallis[3], Helen Marr[3], Scott Marshall[4], Nick Bown[5], Elaine Willmore[1], John Lunec[1]

[1] Northern Institute for Cancer Research, Newcastle University, Newcastle upon Tyne, United Kingdom

[2] Faculty of Medical Sciences, Newcastle University, Newcastle upon Tyne, United Kingdom

[3] Department of Haematology, Freeman Hospital, The Newcastle upon Tyne NHS Foundation Trust, Newcastle upon Tyne, United Kingdom

[4] Department of Haematology, City Hospitals Sunderland NHS Trust, Sunderland, United Kingdom

[5] Northern Genetics Service, Institute of Genetic Medicine, Newcastle upon Tyne, United Kingdom

Running Title: MDM2 inhibition in chronic lymphocytic leukemia

Corresponding author:

Professor John Lunec

Gillespie Professor of Molecular Oncology

Northern Institute for Cancer Research, Paul O'Gorman Building, Newcastle University, Framlington Place, Newcastle upon Tyne NE2 4HH, United Kingdom

Email: john.lunec@ncl.ac.uk

Telephone: +44 (0) 191 208 4420

Fax: +44 (0) 191 208 4301

COMPETING INTERESTS

All authors declare there are no competing financial interests in relation to the work described. This study was supported by Bloodwise (grant # 13034), the JGW Patterson Foundation (grant # BH152495) and the Newcastle Healthcare Charity (grant # BH152694).

ABSTRACT

Chronic lymphocytic leukemia is a clinically heterogeneous haematological malignancy which is ~90% *TP53* wild-type at diagnosis. As a primary repressor of p53, targeting of mouse double-minute-2 homolog (MDM2) is an attractive therapeutic approach for non-genotoxic reactivation of p53. Since discovery of the first MDM2 inhibitor, Nutlin-3a, newer potent and bioavailable compounds have been developed. Here, we tested the second-generation MDM2 inhibitor, RG7388, in patient-derived chronic lymphocytic leukemia cells and normal cells, examining its effect on the induction of p53-transcriptional targets. RG7388 potently decreased viability in p53-functional chronic lymphocytic leukemia cells whereas p53-non-functional samples were more drug-resistant. RG7388 induced a pro-apoptotic gene expression signature with upregulation of p53-target genes involved in the intrinsic (*PUMA, BAX)* and extrinsic (*TNFRSF10B, FAS)* pathway of apoptosis, as well as *MDM2*. A slight induction of *CDKN1A* was observed and upregulation of pro-apoptotic genes dominated, indicating that chronic lymphocytic leukemia cells are primed for p53-dependent apoptosis. Consequently, RG7388 led to a concentration-dependent increase in caspase-3/7 activity and cleaved PARP. Importantly, we observed a preferential pro-apoptotic signature in chronic lymphocytic leukemia cells but not in normal blood and bone marrow cells, including CD34+ haematopoietic cells. These data support the further evaluation of MDM2 inhibitors as a novel additional treatment option for patients with p53-functional chronic lymphocytic leukemia.

INTRODUCTION

Chronic lymphocytic leukemia (CLL) is the most prevalent B-cell malignancy in adults and is marked by an extremely heterogeneous clinical course.[1-3] CLL is characterized by a clonal expansion of CD19+/CD5+ B-cells in the blood, bone marrow and lymphoid tissues.[1-3] Malignant B-lymphocytes accumulate partly due to activation of B-cell receptor (BCR) signalling leading to increased proliferation and inhibition of apoptosis.[3] In addition to BCR signalling, CLL cells are supported by the tumour microenvironment, including extensive cytokine and chemokine signalling with T-cells, myeloid cells, and stromal cells.[4-7]

Despite improvements in CLL patient response rates using chemo-immunotherapy and BCR-antagonists, CLL remains incurable.[8,9] In particular, the identification of new agents that interfere with the survival of CLL cells by promoting their apoptosis is one critical approach to improve therapeutic outcome.[10,11] In fact, several studies have demonstrated that the anti-apoptotic BCL2 protein is highly expressed in CLL and inhibits the activity of pro-apoptotic BH3-only family members, such as PUMA.[12-14] Therefore, drugs that can enhance expression of these pro-apoptotic BH3-only proteins might represent a clinically relevant therapeutic option for CLL.

The variable clinical course of CLL is driven, at least in part, by molecular heterogeneity which is underscored by the variety of genetic lesions observed, from classical markers of CLL to new genetic lesions uncovered by whole-genome and whole-exome sequencing.[15-19] Among the genetic lesions identified, *TP53* deletions and/or mutations are restricted to ~10% of CLL cases at diagnosis and are associated with decreased survival and clinical resistance to chemotherapeutic treatment.[15,16] Given the low prevalence of *TP53* defects at diagnosis, the majority of CLL patients retain a functional p53, and in these patients the possibility of activating p53 should be explored as a therapeutic strategy.

Owing to the central role of p53 in preventing aberrant cell proliferation and maintaining genomic integrity, there is an increasing interest in developing pharmacological strategies aimed at manipulating p53 in a non-genotoxic manner, maximizing the selectivity and efficiency of cancer cell eradication.[20,21] The levels and activity of functional p53 are mainly regulated through direct interaction with the human homolog of the murine double-minute 2 (MDM2) protein.[22,23] MDM2 is an E3 ubiquitin ligase which controls p53 half-life *via* ubiquitin-dependent proteasomal degradation.[22] In response to cellular stress, the p53-MDM2 interaction is disrupted and p53 undergoes post-translational modifications on multiple sites to promote transcription of target genes that trigger cell-cycle arrest, apoptosis and/or cell senescence.[20-23] Since the discovery of the first selective small molecule MDM2 inhibitor, Nutlin-3a, newer compounds have been developed with increased potency and improved bioavailability.[24,25] These non-genotoxic compounds bind to MDM2 in the p53-binding pocket with high selectivity and can release p53, leading to effective stabilization of the protein and activation of the p53 pathway.[24,25] Initial preclinical and clinical studies have demonstrated promising efficacy of this class of drugs in a number of p53 wild-type adult and paediatric cancers, as single agents or in combination with other targeted therapies.[26-34] However, the contribution of transcription-dependent pathways to the p53-mediated response in CLL has not been systematically explored, and, importantly, the effect of p53-reactivation and the p53 gene expression signature in normal cells implicated in the dose limiting haematological toxicity is yet to be elucidated.

In this study, we compared the effect of a second-generation and clinically relevant MDM2 inhibitor, RG7388, in patient-derived primary CLL cells and normal blood and bone marrow cells, including CD34+ hematopoietic progenitors, and report the contrasting transcriptional induction profile of p53-target genes and consequent preferential pro-apoptotic responses of CLL cells to RG7388 exposure, compared with normal haematopoietic cells.

METHODS

Patients and cell isolation

Peripheral-blood samples (n=55) from CLL patients (Table S1) were collected in EDTA-coated tubes. Informed consent was obtained in accordance with the Declaration of Helsinki, and with approval obtained from the NHS Research Ethics Committee. CLL patient samples are collected and stored under the auspices of the Newcastle Academic Health Partners Biobank (http://www.ncl.ac.uk/biobanks/collections/nbrtb/). CLL diagnosis was made according to the IWCLL-164 NCI 2008 criteria.[35]

Normal peripheral blood mononuclear cells (PBMCs, n=6), bone marrow mononuclear cells (BMMCs, n=5) and CD34+ haematopoietic stem cells (n=3) were isolated from healthy donors. Details on isolation and culture of leukemic and normal cells are in the Supplementary Methods.

Reagents

The small-molecule MDM2 inhibitor RG7388 was custom synthesised as part of the Newcastle University/Astex Pharmaceuticals Alliance and CRUK Drug Discovery Programme at the Northern Institute for Cancer Research, Newcastle University. RG7388 was dissolved in DMSO to make a 10 mM stock solution and stored in small aliquots at −20 °C.

Nutlin-3a was purchased from Cambridge Bioscience (Cambridge, UK), Ibrutinib from Axxora (Enzo Life Sciences, Exeter, UK), Venetoclax (ABT199) from Selleckchem, Absource Diagnostics (Munich, Germany).

Functional assessment of the p53 pathway

The p53 functional status of CLL samples was determined by observing the modulation of p53 and transcriptional target gene protein products, MDM2 and p21, following short-term exposure to MDM2 inhibitors.[36] The *TP53* mutational status of CLL samples was also assessed by Next Generation Sequencing (Roche 454 GS FLX and Illumina MiSeq platforms) in 54/55 samples. The presence of 17p deletion was assessed by FISH and/or MLPA analysis in 54/55 samples. In one case (CLL 0255), we were unable to perform DNA analysis, therefore the p53 functional status was evaluated *in vitro* using a short-term exposure of the CLL cells to MDM2 inhibitors, and this sample was identified as p53-non-functional.

***Ex vivo* cytotoxicity assay**

$5x10^6$ cells/ml in 100µl of medium per well of a 96-well plate were exposed to a range of concentrations of RG7388 for 48 hours. Cytotoxicity was assessed by XTT Cell Proliferation Kit II (SigmaAldrich, UK) as detailed in the Supplementary Methods.

Western blot analysis

$5x10^6$ cells/ml were seeded in 1ml per well of a 24-well plate and exposed to a range of concentrations of RG7388. Cells were harvested and lysed at 6 and 24 hours. Protein concentration was measured using a Pierce™ BCA Protein Assay Kit (Thermo Fisher Scientific, UK). A detailed protocol is in the Supplementary Methods.

qRT-PCR gene expression analysis

$5x10^6$ cells/ml were seeded in 2ml per well of a 12-well plate and exposed to a range of concentrations of RG7388 for 6 and 24 hours. Total RNA was isolated using RNeasy Mini kit

(Qiagen, Manchester, UK). Concentration and purity of the RNA were measured using a NanoDrop ND-1000 Spectrophotometer. RNA was reverse-transcribed with a High-Capacity cDNA Reverse Transcription Kit (Thermo Fisher Scientific, UK). Relative quantification of *BAX, CKDN1A, MDM2, PUMA (BBC3), FAS, FDXR, GADD45A, TNFRSF10B, ZMAT3, TP53INP1* and *WIP1/PPM1D* mRNA expression was performed by qRT-PCR based on SybrGreen chemistry using an Applied Biosystems QuantStudio™ 7 Real-Time PCR System (Applied Biosystems, UK). Each sample was analysed in triplicate using *GAPDH* as a house-keeping control. The relative expression of each gene, expressed as fold-change, was calculated by the $2^{-\Delta\Delta Ct}$ method and each sample was normalized to its DMSO-treated matched sample. Validated primer sequences are available in Table S2. The gene panel selected for this study was based on the results of a recent phase I trial of the MDM2 inhibitor RG7112[29] and published data from our group reporting the effect of MDM2 antagonists in different cancer cell lines.[31,34]

Additional analysis of a panel of anti-apoptotic genes (*BCL2, MCL1* and *BCL2L1*(BCL-XL)), plus the pro-apoptotic genes *PMAIP1*(NOXA) and *BCL2L11*(BIM) (Table S2) was also performed on a subset of samples.

Apoptosis assay

$5x10^5$ cells/well were seeded in 96-well plates and exposed to increasing concentrations of RG7388 for 24 hours. Caspase 3/7 activity (Caspase-Glo® 3/7 Assay, Promega, UK) was assessed as detailed in the Supplementary Methods. Apoptosis was also determined by examining cleaved PARP by western blot.

Co-culture and stimulation of CLL cells with CD40L-expressing cells

CLL cells were cultured on a monolayer of CD40L-expressing mouse fibroblasts and exposed to RG7388 as detailed in the Supplementary Methods.

Cell cycle analysis of CD34+ haematopoietic stem cells

CD34+ cells were exposed to RG7388 for 24 hours and cell cycle distribution was evaluated as detailed in the Supplementary Methods.

Statistical analysis

Statistical analysis was performed using GraphPad Prism v6 (GraphPad Software Inc). Statistical differences between groups were evaluated by paired Student's t-test or Mann–Whitney test. Correlations were analysed by Pearson's rank correlation test. p-values<0.05 were considered statistically significant.

Hierarchical cluster analysis of the Euclidean distances of gene expression levels was carried out using the R pheatmap package.[37] The subsequent group LC_{50} comparison was performed using ANOVA by parametric tests with Holm-Sidaks's correction for multiple comparisons between groups.

RESULTS

***TP53* genomic status of CLL samples**

Supplementary Table S1 provides details of the *TP53* mutations, including coding region position and amino acid changes as well as del17p status. The mutations detected were mostly (8/9 CLL samples) in the DNA binding domain (amino acids 102-292) and the remaining case (CLL273) had a double mutation in the C-terminal tetramerisation domain. All mutations were deleterious leading to loss of function.

The MDM2 inhibitor RG7388 induces functional stabilisation of p53 in CLL cells

We assessed protein expression of p53, as well as p53-regulated downstream targets, in patient-derived CLL cells by western blot, following incubation with RG7388. Inhibition of MDM2 by RG7388 blocked ubiquitin-mediated degradation of p53, leading to its accumulation. In p53-functional CLL samples, RG7388 led to a concentration-dependent stabilisation of p53, with subsequent activation of downstream proteins, p21 and MDM2 (Figure 1A). The accumulation of p53 was detectable in all p53-functional CLL samples as soon as 6 hours after commencement of treatment and increased at 24 hours (Figure 1A). In the 30 p53-functional CLL samples analysed, RG7388 increased p21 protein expression in 77% of cases and led to a detectable auto-regulatory feedback increase in expression of MDM2 in 85% of cases. The activation of these two downstream targets occurred in a concentration- and time-dependent manner (Figure 1A). Conversely, in p53-non-functional CLL samples, we found no stabilisation of p53 nor induction of MDM2 and p21 after treatment with RG7388, even up to 10 μM (Figure 1B). The increased potency against CLL cells of the second generation MDM2 inhibitor RG7388 compared with Nutlin-3a is shown in Figure 1C.

RG7388 induces a predominantly pro-apoptotic gene expression signature in CLL cells

We used qRT-PCR to study the expression of 11 known p53 transcriptional target genes in 26 CLL samples after treatment with RG7388. In p53-functional CLL samples, MDM2 inhibition by RG7388 led to a concentration- and time-dependent upregulation of p53-transcriptional targets (exemplified by CLL 0262 and 0267, Figure 2A). No change in gene expression was identified in p53-non-functional samples (exemplified by CLL 0261, Figure 2B).

The results for the 24 p53-functional CLL samples are summarised in Figure 3A, which demonstrates the concentration-dependent nature of the fold-change in gene expression. The results for the 2 p53-non-functional CLL samples are shown in Figure 3B. In p53-functional samples, 6 genes were induced (≥2-fold) above baseline in response to 1 μM RG7388 for 6 hours, all of which are known to be directly regulated by p53 (Figure 3C). We observed a mean 8.5-fold increase in *PUMA*, 5.1-fold in *MDM2*, 3.8-fold in *BAX*, 2.7-fold in *TNFRSF10B*, 2.6-fold in *FAS*, 2.2-fold in *WIP1*, and 1.6-fold in *CDKN1A* (Figure 3C). Thus, only a slight upregulation of *CDKN1A*, encoding the p21 cyclin-dependent kinase inhibitor, was observed and induction of pro-apoptotic genes dominated. Additional analysis of a panel of anti-apoptotic genes (*BCL2, MCL1* and *BCL2L1*(BCL-XL)), plus the pro-apoptotic genes *PMAIP1*(NOXA) and *BCL2L11*(BIM) showed no significant changes in mRNA expression compared with the large change in *PUMA* mRNA (Figure 3D). Western blot analysis confirmed that induction of PUMA protein by RG7388 treatment could be detected in CLL samples (Figure S1 A).

As would be expected on bulk analysis, CLL 0269, harbouring a small subclonal 17p deletion (22% of nuclei), but no evidence of a *TP53* mutation, nevertheless showed functional stabilisation of p53 by RG7388 (Figure S2 A) with subsequent upregulation of p53 target genes (Figure S2 B), apoptosis (Figure S2 C) and moderate cytotoxicity (Figure S2 D).

To identify functional subgroups based on their gene expression induction after exposure to 1μM RG7388, we performed unsupervised cluster analysis of CLL samples based on the fold-change of the 11 p53-transcriptional targets. This analysis showed a significant segregation of p53-functional CLL samples into three groups (defined as Group A, B and C), where Group A showed a lower induction of p53-targets compared to the other samples, despite its wild-type p53 genomic and functional status (Figure 4A). The three groups also

showed different mean RG7388 LC_{50} values and, in particular, group A showed a significantly higher mean LC_{50} than Group B and C (Figure 4B-C).

RG7388 induces a concentration-dependent cytotoxic effect on CLL cells

To investigate the effect of RG7388 on cell viability, 55 CLL samples (Table S1) were incubated with RG7388 and assayed for viability after 48 hours using an XTT assay. Although caspase activity indicating the triggering of apoptosis can be seen at 24hrs, it takes a further 24hrs for the loss of viability measured by XTT assay to become fully evident (Figure S1 B). RG7388 induced a concentration-dependent cytotoxic effect on CLL cells exhibiting functional p53 responses (examples shown in Figure 5A) but not in those without a functional p53 response (Figure 5B). Overall, *TP53*-wild type samples had a median LC_{50} of 0.37 µM (Figure 5C). As expected, CLL samples with mutated/deleted *TP53* were much more drug-resistant (median LC_{50}=4.1 µM) (Figure 5C, which also details *TP53* mutant allele frequency). Interestingly, three samples harbouring a subclonal *TP53* mutation (variant allele frequency <50%) in the absence of del17p showed a decrease in cell viability (RG7388 LC_{50}<1 µM). All other mutant samples, including del17p cases, had LC_{50}>1 µM (Figure 5C). In CLL 0255 we were unable to perform DNA analysis (see 'Materials and Methods'). This sample was functionally defective (Figure 1B) and hence included in Figure 5C in the *TP53*-mutant subgroup (LC_{50}=8.4 µM).

Notably, among *TP53*-wild type samples, a small subset showed an intermediate response (1 µM<LC_{50}<10 µM, n=5) or resistance (LC_{50}>10 µM, n=3) to RG7388 (Figure 5D). Importantly, wild-type *TP53* cells from patients of different CLL risk subgroups were similarly sensitive to RG7388. There was no significant difference in LC_{50} between Binet stage A and C (Figure S3 A), mutated or unmutated *IGHV* genes (Figure S3 B) or cases with high-risk cytogenetic abnormalities such as 11q deletion and trisomy 12 (Figure S3 C).

Given the importance of microenvironmental stimuli on survival and activation of CLL cells as well as response to therapy, we next sought to evaluate the effect of RG7388 in CD40L/IL4-stimulated CLL cells. We found that co-culturing CLL cells with CD40L-expressing fibroblasts and IL4 significantly reduced the spontaneous apoptosis associated with CLL cells and induced their proliferation. Importantly, RG7388 abrogated the protection induced by CD40L/IL4 and inhibited proliferation of stimulated CLL cells (Figure S4 A). Proliferating CLL cells cultured on the CD40L-expressing layer for 96 hr were exposed to RG7388 and cell counting 48 hours after exposure revealed a concentration-dependent suppression of cell growth with GI_{50} values in the nM range (Figure S4 B-C). Furthermore, p53 stabilisation and induction of p53 targets was much higher in stimulated-CLL cells than their unstimulated counterpart, suggesting that p53 anti-tumour activity can be rescued even in CLL cells protected by their microenvironment (Figure S4 D-E). Interestingly, a higher upregulation of *CDKN1A* and *MDM2* and a lower induction of *PUMA* was measured in stimulated-CLL cells compared to unstimulated cells (Figure S4-F), along with no induction of cleaved PARP (Figure S4 D-E), suggesting that RG7388 may elicit a preferential growth-arrest rather than apoptosis in CD40L/IL4-stimulated CLL cells and it can disrupt signalling from the microenvironment that leads to *in vivo* CLL cell proliferation.

RG7388 induces apoptosis in p53-functional CLL

To further investigate the mechanism of RG7388 cytotoxicity, induction of apoptosis was assessed by measuring caspase 3/7 activity and cleaved PARP expression. At 24 hours, RG7388 increased Caspase 3/7 activity in p53-functional cells (Figure 6A), whereas no increased Caspase 3/7 activity was observed in p53-non-functional CLL samples (Figure 6B). To corroborate this, we also measured cleaved PARP expression by western blot and found

that RG7388 increased expression of the 89 kDa cleaved PARP isoform in p53-functional CLL samples (Figure 6C) but not in p53-non-functional samples (Figure 6D).

Gene expression signature and response to RG7388 in normal cells and CLL cells is markedly distinct

A concern of p53-reactivating therapies is the effect on normal cells. It has been suggested that MDM2 inhibitors might activate different cellular responses in normal and tumour cells.[38-41] To investigate this specifically and in more mechanistic detail in the context of CLL, we tested the effect of RG7388 on normal cells implicated in the dose limiting haematological toxicity of MDM2 inhibitors. We isolated PBMCs, BMMCs and CD34+ haematopoietic stem cells from healthy donors and analysed the transcriptional profile of p53-target genes and the cytotoxic response to RG7388.

As expected, p53 transcriptional targets were induced by RG7388 in all normal cell types. However, in contrast to p53-functional CLL cells, which displayed a strong pro-apoptotic gene signature (Figure 2), MDM2 inhibition led to a significant and preferential upregulation of *MDM2* in PBMCs (Figure 7A), BMMCs (Figure 7B) and CD34+ hematopoietic stem cells (Figure 7C).

We then compared the data obtained from CLL cells (Figure 3-6) with the effects seen in normal cells. Treatment with 1 μM RG7388 for 6 hours induced the pro-apoptotic gene *PUMA* in p53-functional CLL cells but not in p53-non-functional CLL or normal BMMCs. Only a relatively small induction of *PUMA* was observed in normal PBMCs and CD34+ cells (Figure 8A). However, for *MDM2*, induction was highest in normal CD34+ cells and comparable for normal PBMCs and p53-functional CLL cells (Figure 8B).

Furthermore and strikingly, *MDM2* upregulation dominated over the other target genes in normal cells (Figure 7) in contrast to the dominance of *PUMA* in CLL cells (Figure 2). Of

additional importance, the mean induction of *CDKN1A* was higher in normal PBMCs than in p53-functional CLL cells (Figure 8C), suggesting the reactivation of p53 in normal circulating blood cells by MDM2 inhibitors does not activate a cell-death signal.

Importantly, the RG7388 LC_{50} values were always >3 μM for normal PBMCs and BMMCs, and >2 μM for CD34+ cells (Figure 8D), whereas the LC_{50} values were <0.4 μM in p53-functional CLL cells (Figures 5C, 8D). We also found that when normal BMMCs and PBMCs were treated with RG7388, the increase of caspase 3/7 activity was significantly lower than that observed in p53-functional CLL cells (Figure S5). The small amount of caspase activity and cell killing induced by RG7388 in PBMCs likely represents the effect on the small component of normal B-cells, whilst T-cells remain unaffected, as previously reported for Nutlin-3a response.[42]

Also of note, positively-selected CD34+ cells (Figure S6 A, B) incubated with RG7388 for 24 hours showed a reduced proportion of cells in S-phase together with an increase in G0/G1 (Figure S6 C). There was also a small increase of cells in the subG1 phase of the cell cycle (Figure S6 D).

RG7388 induces cytotoxicity independently of *MDM2* and *PUMA* basal expression or upregulation

MDM2 has been reported to be overexpressed in 50-70% of CLL cases.[43,44] However, the role of MDM2 overexpression in p53 dysfunction remains controversial, and it has been suggested that p53 activation in CLL cells is largely unaffected by variations in basal levels of MDM2.[45,46] Moreover, it remains unclear whether basal levels of the crucial apoptotic regulator *PUMA* may serve as a biomarker of response to MDM2 inhibitors. To examine whether *MDM2* or *PUMA* basal expression impacts on the cytotoxic effect of RG7388, we measured the basal mRNA levels of these two transcripts by qRT-PCR. The basal Ct values

of *MDM2* and *PUMA* were generally lower, and hence expression higher, in primary CLL samples than in normal BMMCs (Figure S7 A, B). However, mean *MDM2* basal Ct values were significantly higher in CLL cells compared to normal PBMCs (Figure S7 A), whereas *PUMA* basal expression was comparable in CLL and normal PBMCs (Figure S7 B). Basal *MDM2* and *PUMA* Ct values did not significantly differ between CLL samples and CD34+ cells. The basal expression of *MDM2* and *PUMA* was also similar between RG7388-sensitive responders (LC_{50}<1 μM) and intermediate/resistant CLL samples (LC_{50}>1 μM) (Figure S7 C,D). Moreover, we found no correlation between basal *MDM2* or *PUMA* expression and RG7388 LC_{50} values, (Figure S7 C,D), supporting the previous observations that variation in MDM2 expression does not impact the functional activation of p53 and Nutlin 3a-induced cell death in CLL.[45,46]

In our cohort, the *MDM2* and *PUMA* fold-changes induced by 1 μM RG7388 at 6 hours also alone do not correlate with the LC_{50} values (Figure S8 A, B), suggesting that additional factors are important determinants of MDM2 inhibitor-induced cytotoxicity in CLL.

Combination treatments with RG7388

Although not the primary aim of this paper, we include some initial combination data. For ABT199 (venetoclax) and RG7388 there is an additive response, but for *ex vivo* treatment there was no additional benefit of adding Ibrutinib to RG7388 (Figure S9).

DISCUSSION

Owing to the central role of p53 in preventing aberrant cell proliferation and maintaining genomic integrity, as well as in the response to chemotherapy, there is an increasing interest in the development of pharmacological strategies aimed at activating p53.[20,21] These strategies include compounds that rely on non-genotoxic activation of p53 by preventing it

from being inhibited and targeted for degradation by MDM2, thus stabilising p53 and activating its transcriptional activity to promote p53-induced apoptosis.[20,21,24,25] Here, we provide a strong rationale for the future evaluation of MDM2 inhibitors for CLL therapy, based on our observations that CLL cells are particularly primed for p53-dependent apoptosis compared with normal PBMCs, BMMCs and CD34+ hematopoietic stem cells. We showed that RG7388 activates p53 and restores p53-transcriptional activity, inducing a characteristic dominant pro-apoptotic gene expression signature of p53-target genes selectively in CLL cells. Overall, no significant induction of transcriptional targets was observed in p53-non-functional samples, consistent with specificity of RG7388 for p53 wild-type cells. However, a CLL sample harbouring a subclonal 17p deletion in 22% of nuclei showed functional activation of p53 and induction of cell death in response to RG7388. This suggests that in the presence of low subclonal levels of p53 loss, the predominant p53-functional cell population can still respond to non-genotoxic activation of p53 and patients with subclonal *TP53* abnormalities could still benefit from treatment with new generation MDM2 inhibitors, especially in combination with other p53-independent targeted therapies.

Moreover, RG7388 triggered apoptosis in CLL cells. This effect was dependent, in the majority of samples, on the presence of functional p53. CLL samples with predominantly mutated, non-functional p53 did not show apoptotic induction. As a consequence of upregulation of apoptotic genes and activation of apoptosis, RG7388 significantly decreased the cell viability of p53-functional CLL samples, but CLL samples that displayed non-functional p53 on western blot and mutated/deleted *TP53* showed a greater resistance. However, in the *TP53*-mutant subgroup, three samples harbouring subclonal *TP53* mutations showed an LC_{50} value lower than 1 μM, indicating significantly decreased cell viability upon exposure to RG7388. This finding is in line with the results of a recent phase I clinical trial evaluating the effect of the earlier generation MDM2 inhibitor RG7112 in leukemia.[29] This

included a small number of heavily pre-treated CLL patients for which RG7112 showed clinical activity, with evidence of induction of PUMA and apoptosis in a patient with CLL whose white blood count decreased by >50%.[29] Among RG7112-treated patients, the investigators reported two patients with *TP53* mutant leukaemic cell samples who exhibited a clinical response.[29]

Interestingly, among *TP53*-wild type CLL samples, we identified a small subset that showed intermediate response or resistance to RG7388 treatment, suggesting that *TP53* mutational status is not the only determinant of response to MDM2 antagonists and other biomarkers should be sought. In fact, in addition to p53 dysfunction resulting from *TP53* mutations and/or deletions, human cancers may display p53 suppression as a consequence of upregulation of MDM2 expression.[47] MDM2, which can enhance tumorigenic potential and resistance to apoptosis, has been also reported to be overexpressed in 50-70% of CLL cases[43,44], therefore it is reasonable to hypothesize that aberrant expression of *MDM2* could be an indicator of response to MDM2 inhibitors. However, in our study the basal mRNA expression of *MDM2* was not significantly different between RG7388-sensitive responders (LC_{50}<1 μM) and more resistant CLL samples (LC_{50}>1 μM). Moreover, we found no significant correlation between basal *MDM2* expression or *MDM2* fold-induction and LC_{50} values, supporting previous observations that MDM2 overexpression does not impact on functional activation of p53 and MDM2 inhibitor-induced cytotoxicity in CLL.[45,46] In contrast, a recent study showed that MDM2 protein expression in blasts may identify AML patients likely to exhibit improved outcomes to RG7388-based therapy.[33] Therefore, in other haematological malignancies, quantification of MDM2 basal levels might be clinically relevant to predict sensitivity to MDM2 inhibitors.

The main concern of p53-reactivating therapies is the effect on normal cells. The activation of functional p53 by MDM2 inhibitors could elicit differing cellular responses to p53

activation in tumour compared to normal cells. However, there is a paucity of data on the effect of new generation MDM2 antagonists on normal cells, especially CD34+ hematopoietic stem cells in which drug-induced cytotoxicity can result in the dose-limiting cytopenia that has been reported in early clinical trials of these agents. Although some initial studies (using Nutlin-3 and MI-219) suggested that MDM2 inhibition results in different cellular responses in normal and tumour cells,[38-41] the pattern of p53-dependent gene expression induced by MDM2 inhibition in primary CLL cells *versus* normal blood cells has not been investigated.

Here, we show for the first time that the expression of p53-target genes in response to RG7388 in normal peripheral blood and bone marrow cells (including positively-selected CD34+ haematopoietic progenitors) is distinct to that in primary CLL cells. Induction of the pro-apoptotic *PUMA* gene after RG7388 treatment was the dominant response in CLL cells. This contrasted with the response of normal blood cells and CD34+ hematopoietic stem cells, where activation of apoptosis was weak or absent and upregulation of the negative feedback regulator *MDM2* dominated over pro-apoptotic target genes. Interestingly, the induction of *CDKN1A* was also higher in normal PBMCs than in p53-functional CLL cells, suggesting that reactivation of p53 in normal, circulating blood cells by MDM2 inhibitors fails to elicit the predominant cell-death signal seen in CLL cells. In CD34+ cells, gene expression and cell cycle distribution changes also suggest that cell-cycle arrest and an effective re-establishment of the MDM2-p53 negative feedback loop, rather than apoptosis, might be the main effects elicited by RG7388. These findings provide a mechanistic rationale for observations using first-generation MDM2 antagonists that have suggested a predominant, reversible growth arrest as a primary response of normal cells to MDM2 inhibition.[38-41] Consistent with this, activation of Caspase 3/7 and cytotoxicity upon exposure to RG7388 was significantly lower in normal blood and bone marrow cells, compared with primary CLL cells.

Although p53 is activated by MDM2 inhibitors in both normal and tumour cells with functional p53, the gene expression signature and the cytotoxic effect induced by p53 activation in these two settings is markedly distinct, which translates into different cell fates and provides a therapeutic index with significant implications for the potential applications of MDM2 inhibitors as new anticancer agents. Of additional importance, RG7388 also effectively blocked proliferation signals provided externally to CLL cells *in vitro* to model the microenvironment using CD40L and IL4, which are crucial *in vivo* stimuli for proliferation of leukemic cells in lymph nodes and bone marrow.

IgM stimulation of B-cell receptor signalling has been reported to increase protein levels of MCL1, but not BCL2, and to promote the survival of CLL cells.[48] Because of the importance of B-cell receptor signalling in CLL it would be interesting to explore the effect of IgM and/or IL4 stimulation on the response of CLL cells to MDM2 inhibitors, with and without specific inhibitors of BCL2 and MCL1. IgM stimulation of B-cell receptor signalling would also provide a potential *ex vivo* model simulating the lymph node microenvironment for investigating combination treatments with Ibrutinib.

We cannot rule out that conformational changes in BAX may be important, although *BAX* expression changes little compared to the clear large changes in *PUMA* expression. A transcription-independent p53 role in CLL cell apoptosis, involving direct interaction of p53 with mitochondrial anti-apoptotic proteins such as BCL2 has been suggested.[42] We favour a model in which p53 transcription dependent and independent mechanisms work hand in hand. Stabilisation of p53 and upregulation of p53 transcriptional target genes, including predominantly pro-apoptotic genes, particularly PUMA, are the earliest and necessary events in the response of CLL cells to MDM2-p53 binding interaction inhibitors. Gene knockout mouse studies show that PUMA is necessary for apoptosis and p53 induction on its own is not sufficient. Studies on *BAX* nullizygous mice concluded that PUMA provides the critical

link between p53 and BAX and is both necessary and sufficient to mediate DNA damage induced apoptosis.[49] Furthermore *PUMA* knockout studies in mice show recapitulation of virtually all apoptotic deficiency in *p53* knockout mice.[50] It is therefore reasonable to link the major induction of *PUMA* by MDM2 inhibitor treatment of CLL cells with an important role in their sensitivity to the induction of apoptosis by these compounds. The absence of any marked downregulation of BCL family anti-apoptotic gene expression in our current study ruled out suppression of their transcriptional expression as a major contributory mechanism to the response to MDM2 inhibitors.

In considering the therapeutic potential for MDM2 inhibitors in CLL, it should be also emphasized that, despite improvement in patient response rate using chemo-immunotherapy combinations or BCR-antagonists, none of the current therapeutic regimens is curative.[8,9] They are subject to limitations, including the evolution of drug resistance mechanisms. Resistance as a result of mutations in the venetoclax binding domain of BCL2 has been reported in a high proportion of patients who relapse after treatment with venetoclax.[51] Similarly, a high incidence of clonal evolution leading to ibrutinib resistance due to mutations in *BTK* and *PLCG2* have been reported in patients progressing on treatment.[52]

Continued preclinical studies to develop innovative therapeutic strategies for CLL therefore remain a high priority. In particular, new agents promoting CLL cell apoptosis with limited toxicity on normal cells represents an attractive therapeutic strategy for CLL, which is a disease of elderly patients who would benefit from the use of compounds with a therapeutic window associated with minimal effects on normal cells. Moreover, given the clinical heterogeneity of CLL, there is a constant need to identify treatment strategies that can be effective also in the most aggressive subtypes of this disease. In our cohort, RG7388 significantly decreased the viability of CLL cells isolated from patients of different poor prognosis subgroups, including cases with advanced disease stage, cases with unmutated

IGHV genes and cases with 11q deletion and trisomy 12, which are usually more prone to progressive disease. This indicates that inhibiting the p53-MDM2 interaction is a promising treatment strategy to explore for high-risk CLL patients with functional p53.

Taken together, our data demonstrate that MDM2 inhibitors induce a pro-apoptotic response in both low- and high-risk subtypes of CLL patient cells, at doses which show a lesser effect on normal blood cells and hematopoietic stem cells. This therapeutic window supports the clinical evaluation of new generation, non-genotoxic MDM2 inhibitors, used in combined treatment strategies with other targeted therapies for the treatment of CLL.

ACKNOWLEDGEMENTS

This study was supported by Bloodwise (grant # 13034), the JGW Patterson Foundation (grant # BH152495) and the Newcastle Healthcare Charity (grant # BH152694).

The authors would like to gratefully acknowledge Newcastle University/Astex Pharmaceuticals Alliance and CRUK who funded the Drug Discovery Programme at the Northern Institute for Cancer Research, Newcastle University for their support and encouragement.

The authors would also like to thank Jane Cole for recruiting patients and providing clinical information, Dr Kenneth Rankin for providing bone marrow samples, Dr Sally Hall for providing blood samples from healthy donors and all the CLL patients for generously donating samples.

AUTHORSHIP CONTRIBUTIONS

C.C. performed experiments, analysed data and wrote the manuscript. E.A. and L.W. performed experiments. W-Y.L. performed clustering analysis. J.P.W., H.M. and S.M recruited patients and provided clinical information. N.B. analysed cytogenetic abnormalities and provided clinical information. E.W. and J.L. designed the research, secured funding and edited the manuscript.

DISCLOSURE OF CONFLICT OF INTEREST

The authors declare no potential conflicts of interest.

REFERENCES

1. Chiorazzi N, Rai KR, Ferrarini M. Chronic lymphocytic leukemia. N Engl J Med. 2005;352(8):804-815.

2. Müller-Hermelink HK, Montserrat E, Catovsky D, Campo E, Harris NL, Stein H. Chronic lymphocytic leukemia/small lymphocytic lymphoma. In: Swerdlow SH, Campo E, Harris NL, et al. (Eds.), World Health Organization Classification of Tumours, Pathology and Genetics of Tumours of Haematopoietic and Lymphoid Tissues, IARC, Lyon, France: 2008:180–182.

3. Zenz T, Mertens D, Küppers R, Döhner H, Stilgenbauer S. From pathogenesis to treatment of chronic lymphocytic leukaemia. Nat Rev Cancer. 2010;10(1):37-50.

4. Herishanu Y, Perez-Galan P, Liu D, et al. The lymph node microenvironment promotes B-cell receptor signaling, NF-kappaB activation, and tumor proliferation in chronic lymphocytic leukemia. Blood. 2011;117(2):563-574.

5. Kay NE, Wasil T. Survival of chronic lymphocytic leukemia cells: CD40L and the vascular endothelial growth factor (VEGF) connection. Leukemia. 2005;19(4):531-532.

6. Munk Pedersen I, Reed J. Microenvironmental interactions and survival of CLL B-cells. Leuk Lymphoma. 2004;45(12):2365-2372.

7. Herishanu Y, Katz BZ, Lipsky A, Wiestner A. Biology of chronic lymphocytic leukemia in different microenvironments: clinical and therapeutic implications. Hematol Oncol Clin North Am. 2013;27(2):173-206.

8. Badoux XC, Keating MJ, Wang X, et al. Fludarabine, cyclophosphamide, and rituximab chemoimmunotherapy is highly effective treatment for relapsed patients with CLL. Blood. 2011;117(11):3016-3024.

9. Burger JA, Tedeschi A, Barr PM, et al. Ibrutinib as Initial Therapy for Patients with Chronic Lymphocytic Leukemia. N Engl J Med. 2015;373(25):2425-2437.

10. Billard C. Apoptosis inducers in chronic lymphocytic leukemia. Oncotarget. 2014;5(2):309–325.

11. Besbes S, Mirshahi M, Pocard M, Billard C. Strategies targeting apoptosis proteins to improve therapy of chronic lymphocytic leukemia. Blood Rev. 2015;29(5):345-350.

12. Faderl S, Keating MJ, Do KA, et al. Expression profile of 11 proteins and their prognostic significance in patients with chronic lymphocytic leukemia (CLL). Leukemia. 2002;16(6):1045-1052.

13. Robertson LE, Plunkett W, McConnell K, Keating MJ, McDonnell TJ. Bcl-2 expression in chronic lymphocytic leukemia and its correlation with the induction of apoptosis and clinical outcome. Leukemia. 1996;10(3):456-459.

14. Molica S, Dattilo A, Giulino C, Levato D, Levato L. Increased Bcl-2/ bax ratio in B-cell chronic lymphocytic leukemia is associated with a progressive pattern of disease. Haematologica. 1998;83(12):1122-1124.

15. Zenz T, Eichhorst B, Busch R, et al. TP53 mutation and survival in chronic lymphocytic leukemia. J Clin Oncol. 2010;28(29):4473-4479.

16. Dicker F, Herholz H, Schnittger S, et al. The detection of TP53 mutations in chronic lymphocytic leukemia independently predicts rapid disease progression and is highly correlated with a complex aberrant karyotype. Leukemia. 2009;23(1):117-124.

17. Puente XS, Pinyol M, Quesada V, et al. Whole-genome sequencing identifies recurrent mutations in chronic lymphocytic leukaemia. Nature. 2011;475(7354):101-105.

18. Quesada V, Conde L, Villamor N, et al. Exome sequencing identifies recurrent mutations of the splicing factor SF3B1 gene in chronic lymphocytic leukemia. Nat Genet. 2011;44(1):47-52.

19. Rossi D, Rasi S, Fabbri G, et al. Mutations of NOTCH1 are an independent predictor of survival in chronic lymphocytic leukemia. Blood. 2012;119(2):521-529.

20. Chène P. Inhibiting the p53–MDM2 interaction: an important target for cancer therapy. Nat Rev Cancer. 2003;3(2):102-109.

21. Brown CJ, Lain S, Verma CS, Fersht AR, Lane DP. Awakening guardian angels: drugging the p53 pathway. Nat Rev Cancer. 2009;9(12):862-873.

22. Haupt Y, Maya R, Kazaz A, Oren M. Mdm2 promotes the rapid degradation of p53. Nature. 1997;387(6630):296-299.

23. Moll UM, Petrenko O. The MDM2-p53 interaction. Mol Cancer Res. 2003;1(14):1001-1008.

24. Vu B, Wovkulich P, Pizzolato G, et al. Discovery of RG7112: a small-molecule MDM2 inhibitor in clinical development. ACS Med Chem Lett. 2013;4(5):466-469.

25. Ding Q, Zhang Z, Liu J-J, et al. Discovery of RG7388, a potent and selective p53-MDM2 inhibitor in clinical development. J Med Chem. 2013;56(14):5979-5983.

26. Endo S, Yamato K, Hirai S, et al. Potent in vitro and in vivo antitumor effects of MDM2 inhibitor nutlin-3 in gastric cancer cells. Cancer Sci. 2011;102(3):605-613.

27. Drakos E, Singh RR, Rassidakis GZ, et al. Activation of the p53 pathway by the MDM2 inhibitor nutlin-3a overcomes BCL2 overexpression in a preclinical model of diffuse large B-cell lymphoma associated with t(14;18)(q32;q21). Leukemia. 2011;25(5):856-867.

28. Ray-Coquard I, Blay J-Y, Italiano A, et al. Effect of the MDM2 antagonist RG7112 on the P53 pathway in patients with MDM2-amplified, well-differentiated or

dedifferentiated liposarcoma: an exploratory proof-of-mechanism study. Lancet Oncol. 2012;13(11):1133-1140.

29. Andreeff M, Kelly KR, Yee K, et al. Results of the Phase I Trial of RG7112, a Small-Molecule MDM2 Antagonist in Leukemia. Clin Cancer Res. 2016;22(4):868-876.

30. Verreault M, Schmitt C, Goldwirt L, et al. Preclinical Efficacy of the MDM2 Inhibitor RG7112 in MDM2-Amplified and TP53 Wild-type Glioblastomas. Clin Cancer Res. 2016;22(5):1185-1196.

31. Zanjirband M, Edmondson RJ, Lunec J. Pre-clinical efficacy and synergistic potential of the MDM2-p53 antagonists, Nutlin-3 and RG7388, as single agents and in combined treatment with cisplatin in ovarian cancer. Oncotarget. 2016;7(26):40115-40134.

32. Herting F, Herter S, Friess T, et al. Antitumour activity of the glycoengineered type II anti-CD20 antibody obinutuzumab (GA101) in combination with the MDM2-selective antagonist idasanutlin (RG7388). Eur J Haematol. 2016;97(5):461-470.

33. Reis B, Jukofsky L, Chen G, et al. Acute myeloid leukemia patients' clinical response to idasanutlin (RG7388) is associated with pre-treatment MDM2 protein expression in leukemic blasts. Haematologica. 2016;101(5):e185-188.

34. Esfandiari A, Hawthorne TA, Nakjang S, Lunec J. Chemical Inhibition of Wild-Type p53-Induced Phosphatase 1 (WIP1/PPM1D) by GSK2830371 Potentiates the

Sensitivity to MDM2 Inhibitors in a p53-Dependent Manner. Mol Cancer Ther. 2016;15(3):379-391.

35. Hallek M, Cheson BD, Catovsky D, et al. International Workshop on Chronic Lymphocytic Leukemia. Guidelines for the diagnosis and treatment of chronic lymphocytic leukemia: a report from the International Workshop on Chronic Lymphocytic Leukemia updating the National Cancer Institute-Working Group 1996 guidelines. Blood. 2008;111(12):5446-5456.

36. Pozzo F, Dal Bo M, Peragine N, et al. Detection of TP53 dysfunction in chronic lymphocytic leukemia by an in vitro functional assay based on TP53 activation by the non-genotoxic drug Nutlin-3: a proposal for clinical application. J Hematol Oncol. 2013;6:83.

37. Kolde R. pheatmap: Pretty Heatmaps. R package version 1.0.10 https://cran.r-project.org/web/packages/pheatmap/. 2018

38. Stühmer T, Chatterjee M, Hildebrandt M, et al. Nongenotoxic activation of the p53 pathway as a therapeutic strategy for multiple myeloma. Blood. 2005;106(10):3609-3617.

39. Vassilev LT, Vu BT, Graves B, et al. In vivo activation of the p53 pathway by small-molecule antagonists of MDM2. Science. 2004;303(5659):844-848.

40. Shangary S, Qin D, McEachern D, et al. Temporal activation of p53 by a specific MDM2 inhibitor is selectively toxic to tumors and leads to complete tumor growth inhibition. Proc Natl Acad Sci USA. 2008;105(10):3933-3938.

41. Shangary S, Ding K, Qiu S, et al. Reactivation of p53 by a specific MDM2 antagonist (MI-43) leads to p21-mediated cell cycle arrest and selective cell death in colon cancer. Mol Cancer Ther. 2008;7(6):1533-1542.

42. Steele AJ, Prentice AG, Hoffbrand AV, et al. p53-mediated apoptosis of CLL cells: evidence for a transcription-independent mechanism. Blood. 2008;112(9):3827-3834.

43. Haidar MA, El-Hajj H, Bueso-Ramos CE, et al. Expression profile of MDM-2 proteins in chronic lymphocytic leukemia and their clinical relevance. Am J Hematol. 1997;54(3):189-195

44. Konikova E, Kusenda J. Altered expression of p53 and MDM2 proteins in hematological malignancies. Neoplasma. 2003;50(1):31-40.

45. Pettitt AR, Sherrington PD, Stewart G, Cawley JC, Taylor AM, Stankovic T. p53 dysfunction in B-cell chronic lymphocytic leukemia: inactivation of ATM as an alternative to TP53 mutation. Blood. 2001;98(3):814-822.

46. Kojima K, Konopleva M, McQueen T, O'Brien S, Plunkett W, Andreeff M. Mdm2 inhibitor Nutlin-3a induces p53-mediated apoptosis by transcription-dependent and transcription-independent mechanisms and may overcome Atm-mediated resistance to fludarabine in chronic lymphocytic leukemia. Blood. 2006;108(3):993-1000.

47. Senturk E, Manfredi JJ. Mdm2 and tumorigenesis: evolving theories and unsolved mysteries. Genes Cancer. 2012;3(3-4):192-198.

48. Petlickovski A, Laurenti L, Li X, et al. Sustained signaling through the B-cell receptor induces Mcl-1 and promotes survival of chronic lymphocytic leukemia B cells. Blood. 2005;105(12):4820-4827.

49. Wyttenbach A, Tolkovsky AM. The BH3-only protein Puma is both necessary and sufficient for neuronal apoptosis induced by DNA damage in sympathetic neurons. J Neurochem. 2006;96(5):1213-1226.

50. Jeffers JR, Parganas E, Lee Y, et al. Puma is an essential mediator of p53-dependent and -independent apoptotic pathways. Cancer Cell. 2003;4(4):321-328.

51. Blombery P, Anderson MA, Gong JN, et al. Acquisition of the Recurrent Gly101Val Mutation in BCL2 Confers Resistance to Venetoclax in Patients with Progressive Chronic Lymphocytic Leukemia. Cancer Discov. 2019;9(3):342-353.

52. Ahn IE, Underbayev C, Albitar A, et al. Clonal evolution leading to ibrutinib resistance in chronic lymphocytic leukemia. Blood. 2017;129(11):1469-1479.

FIGURE LEGENDS

Figure 1

p53 functional stabilization in CLL cells in response to RG7388.

(A) Western immunoblots showing p53-functional CLL cells either untreated (DMSO) or treated with increasing concentrations of RG7388 (0.1-0.3-1-3 μM) for 6 and 24 hours. Concentration-dependent and time-dependent stabilisation of p53 occurs in p53-functional CLL cells after 6 and 24 hours of incubation with RG7388. Representative examples of 4 independent experiments are shown where both p21 and MDM2 (CLL 0263, CLL 0268), only p21 (CLL 0264) or only MDM2 (CLL 0265) are induced after treatment with RG7388. (B) Western immunoblot showing p53-non-functional CLL cells either untreated (DMSO) or treated with increasing concentrations (1-3-10 μM) of RG7388 for 6 and 24 hours. Lack of stabilisation of p53 or induction of MDM2 and p21 is evident in p53-non-functional CLL cells from patient 0255. High constitutive levels of p53, unchanging after treatment with RG7388, are characteristic of mutant, non-functional p53. The response of cultured wild-type p53 OCI-Ly3 cells to RG7388 is shown as a positive control. (C) Comparison of potency between RG7388 and Nutlin-3a for killing of CLL cells measured by XTT assay for four representative wild-type p53 patient CLL samples; Mean 48hour treatment LC50 values, Nutlin-3a = 2.4μM and RG7388 = 0.18μM.

Figure 2

RG7388 induces mRNA upregulation of pro-apoptotic p53 target genes in CLL cells.

(A) qRT-PCR plots for 2 representative p53-functional samples (CLL 0262, CLL 0267) showing preferential induction of *PUMA* after treatment with increasing concentrations (0.1-0.3-1-3 μM) of RG7388 for 6 and 24 hours. (B) qRT-PCR plots for a representative non-

functional p53 sample (CLL 0261) exposed to increasing concentrations (0.1-0.3-1-3 μM) of RG7388 for 6 and 24 hours.

The results are shown as fold induction relative to DMSO solvent control. Genes induced above the cut-off of 2-fold were considered up-regulated by the treatment. Data are presented as mean ± standard error of mean (SEM) of three repeats.

Figure 3

Apoptosis-related gene expression signature induced by RG7388 in primary CLL cells.

Cells from CLL patients with functional p53 (n=24) were exposed *ex-vivo* to RG7388 for 6 hours. mRNA expression of genes relating to intrinsic apoptosis (*BAX, FDXR, PUMA, TP53INP1*), extrinsic apoptosis (*FAS, TNFRSF10B*), cell cycle arrest (*CDKN1A, ZMAT3, GADDA45A*), and p53 negative autoregulation (*MDM2, WIP1*) was measured in response to RG7388 relative to DMSO solvent control. Genes induced above the cut-off of 2-fold were considered upregulated by the treatment. (A) Expression of p53-target genes in 24 p53-functional samples exposed to increasing concentrations (0.1-0.3-1-3 μM) of RG7388 for 6 hours. Gene induction occurred in a concentration-dependent manner. (B) Expression of p53-target genes in two p53-non-functional samples exposed to increasing concentrations (0.1-0.3-1-3 μM) of RG7388 for 6 hours. No genes were significantly induced by the treatment. (C) Scatter plot showing significant mean induction of *PUMA* (8.5-fold), *MDM2* (5.1-fold), *BAX* (3.8-fold), *TNFRSF10B* (2.7-fold), *FAS* (2.6-fold), and *WIP1* (2.2-fold) in p53-functional CLL samples treated with 1 μM RG7388 for 6 hours. A slight upregulation of *CDKN1A* (1.6-fold) was observed. Data show mean ± standard error of mean (SEM). (D) Scatter plot of qRT-PCR Ct values (cycle number to reach critical threshold) for anti-apoptotic genes *MCL1*, *BCL2* and *BCL-XL*, plus additional Pro-apoptotic genes *NOXA* and *BIM*, in comparison with *PUMA* for n=7 patient CLL samples, showing no significant change

in Ct values and hence mRNA expression between RG7388 treated and untreated (DMSO control) samples except for *PUMA*; Change in Ct for PUMA untreated Vs. PUMA treated at 6 hours p=0.0001, at 24 hours p=0.0066 (paired t-test, n=7).

Figure 4

RNA profiling of p53-trancriptional targets in CLL cells identifies subgroups with different sensitivity (LC50) to RG7388

(A) Unsupervised hierarchical clustering and heat-map of p53 functional CLL samples exposed to 1 μM RG7388 for 6 hours, based on fold-change in expression of an 11-gene panel. The 11 selected p53-transcriptional target genes are listed on the right. Group A, Columns 1-4; Group B, Columns 13-25; Group C, Columns 5-12. (B) CLL patient sample groups identified by the hierarchical clustering analysis compared based on their RG7388 LC_{50} values. (C) Group comparison performed using ANOVA by parametric analysis and applying Holm-Sidak's correction for multiple comparisons. This analysis showed a significant difference in mean RG7388 LC_{50} values between group A and B and between group A and C.

Figure 5

Effect of RG7388 on p53-functional and p53-non-functional CLL cell viability *ex vivo*.

(A) Cytotoxicity curves for three representative p53-functional CLL samples (CLL 0260, CLL 0262, CLL 0268) exposed to increasing concentrations (0.1-0.3-1-3 μM) of RG7388 for 48 hours. RG7388 markedly decreased cell viability as assessed by XTT assay. (B) Cytotoxicity curves for two representative p53-non-functional CLL samples (CLL 0261, CLL 0255) exposed to RG7388 for 48 hours. RG7388 showed no impact on cell viability. (C)

Dot-plot of LC_{50} concentrations for n=45 *TP53* wild type and n=10 *TP53* mutant CLL samples exposed to RG7388 for 48 hours. *TP53* status of these samples was assessed by next generation sequencing and FISH or MLPA. The size of dots indicates the variant allele frequency (VAF). Horizontal bars represent the median. The p-value was assessed by Mann–Whitney test. (D) Dot-plot of LC_{50} concentrations for n=45 *TP53* wild type CLL samples exposed to RG7388 for 48 hours and classified according to their cytotoxic response as sensitive responders (LC_{50}<1 μM), intermediate responders (1 μM <LC_{50}<10 μM) and resistant (LC_{50}>10 μM).

Figure 6

RG7388 leads to a significant dose-dependent increase in apoptosis in p53-functional CLL cells.

(A) Caspase 3/7 activity for three representative p53-functional CLL samples (CLL 0259, CLL 0268, CLL 0276) exposed to increasing concentrations (0.1-0.3-1-3 μM) of RG7388 for 24 hours. (B) Caspase 3/7 activity of a representative p53-non-functional CLL sample (CLL 0261) exposed to increasing concentrations (0.1-0.3-1-3 μM) of RG7388 for 24 hours. Caspase 3/7 activity was measured by a Caspase 3/7 Glo luminescence-based assay and it is represented as % change relative to DMSO solvent control. Data are presented as mean ± standard error of mean (SEM) of three repeats. P-values were calculated by paired t-test.

(C) Western immunoblot for three representative p53-functional CLL samples (CLL 0263, CLL 0264, CLL 0270) showing increased expression of cleaved PARP induced by RG7388 treatment for 24 hours. (D) Western immunoblot for a representative p53-non-functional CLL sample (CLL 0261) showing no change in either full-length or cleaved PARP expression after exposure to RG7388 for 24 hours. Basal levels of cleaved PARP appeared high in this sample (indicative of spontaneous apoptosis) but did not increase with RG7388 treatment.

The Western immunoblots show the full-length pro-form of PARP (116 kDa) and the cPARP cleaved form (89 kDa).

Figure 7

RG7388 preferentially induces *MDM2* mRNA in normal peripheral blood (PBMCs), bone marrow (BMMCs) and CD34+ selected bone marrow cells from healthy donors.

qRT-PCR plots for (A) one representative normal PBMC sample, (B) one representative normal BMMC sample and (C) one representative normal CD34+ sample all showing preferential induction of *MDM2* after treatment with increasing concentrations (0.1-0.3-1-3 μM) of RG7388 for 6 and 24 hours. Data are presented as mean ± standard error of mean (SEM) of at least three repeats.

Figure 8

RG7388 selectively induces *PUMA* expression and cell death in CLL cells compared with normal haematopoietic cells.

(A) *PUMA,* (B) *MDM2* and (C) *CDKN1A* fold changes in mRNA measured by qRT-PCR in p53-functional CLL samples (n=24), p53-non-functional CLL samples (n=2), normal BMMCs (n=5) normal PBMCs (n=6) and normal CD34+ samples (n=3) exposed to 1 μM RG7388 for 6 hours.

(D) Cytotoxic response comparison of normal BMMCs, normal PBMCs, normal CD34+ samples normal and p53-functional CLL samples exposed to RG7388 (0.03-0.1-0.3-1-3 μM) for 48 hours. RG7388 markedly decreased cell viability assessed by XTT assay of p53-functional CLL cells but to a much lesser extent in normal cells.

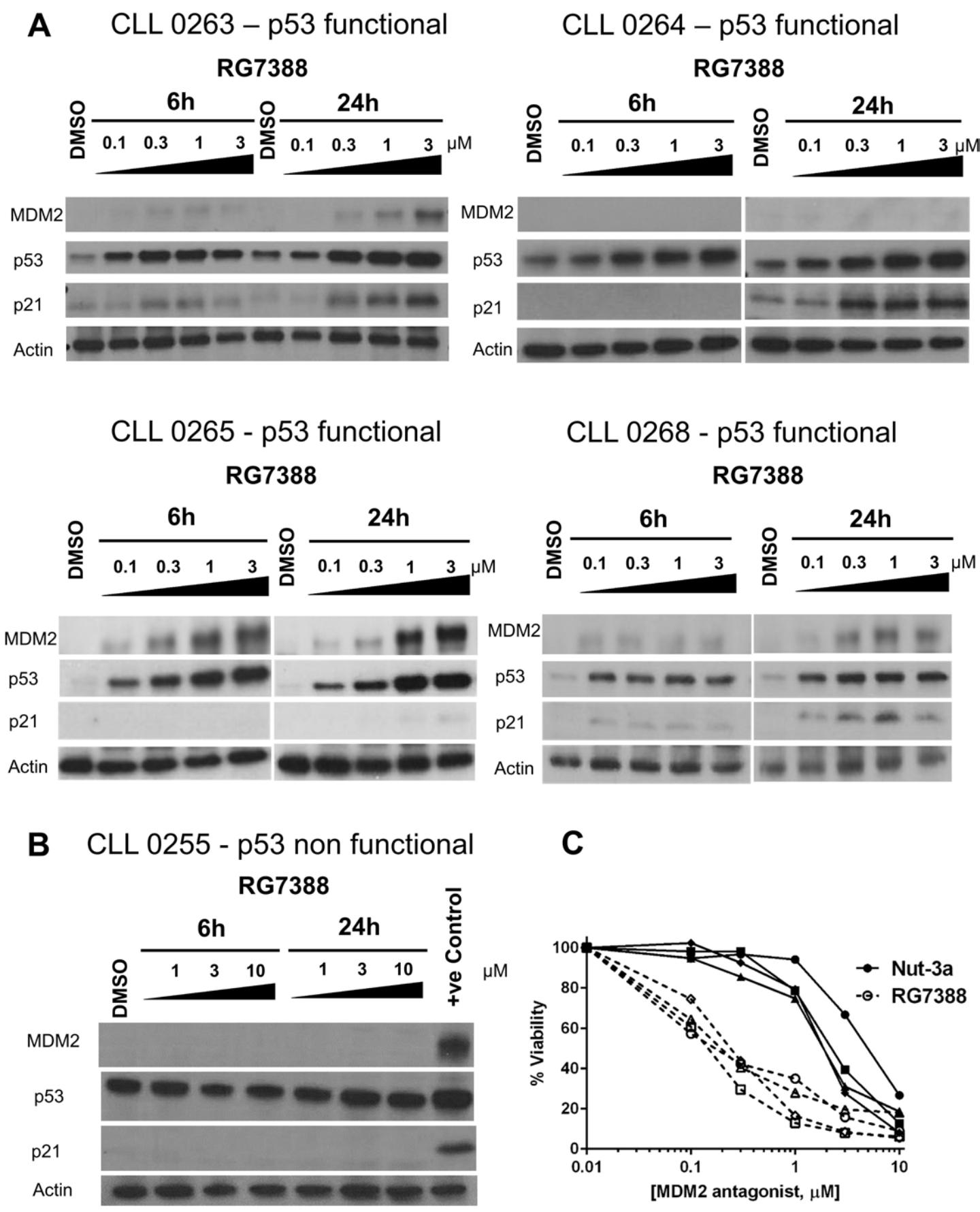

+ve Control: OCI-Ly3 treated with 0.1 µM RG7388 for 24h

Figure 1

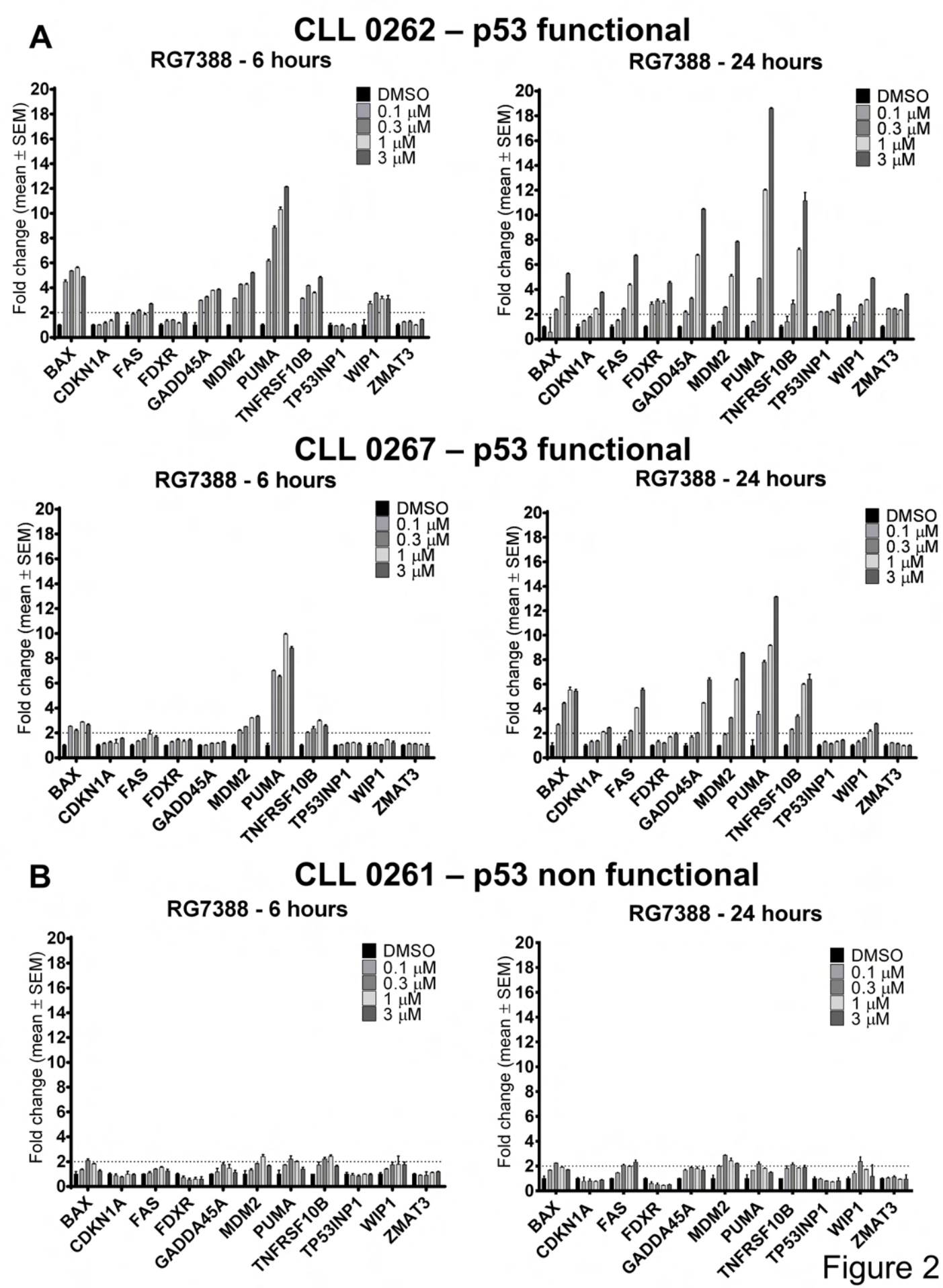
A
CLL 0262 – p53 functional
RG7388 - 6 hours
RG7388 - 24 hours
DMSO
0.1 μM
0.3 μM
1 μM
3 μM
Fold change (mean ± SEM)
BAX
CDKN1A
FAS
FDXR
GADD45A
MDM2
PUMA
TNFRSF10B
TP53INP1
WIP1
ZMAT3
CLL 0267 – p53 functional
RG7388 - 6 hours
RG7388 - 24 hours
B
CLL 0261 – p53 non functional
RG7388 - 6 hours
RG7388 - 24 hours

Figure 2

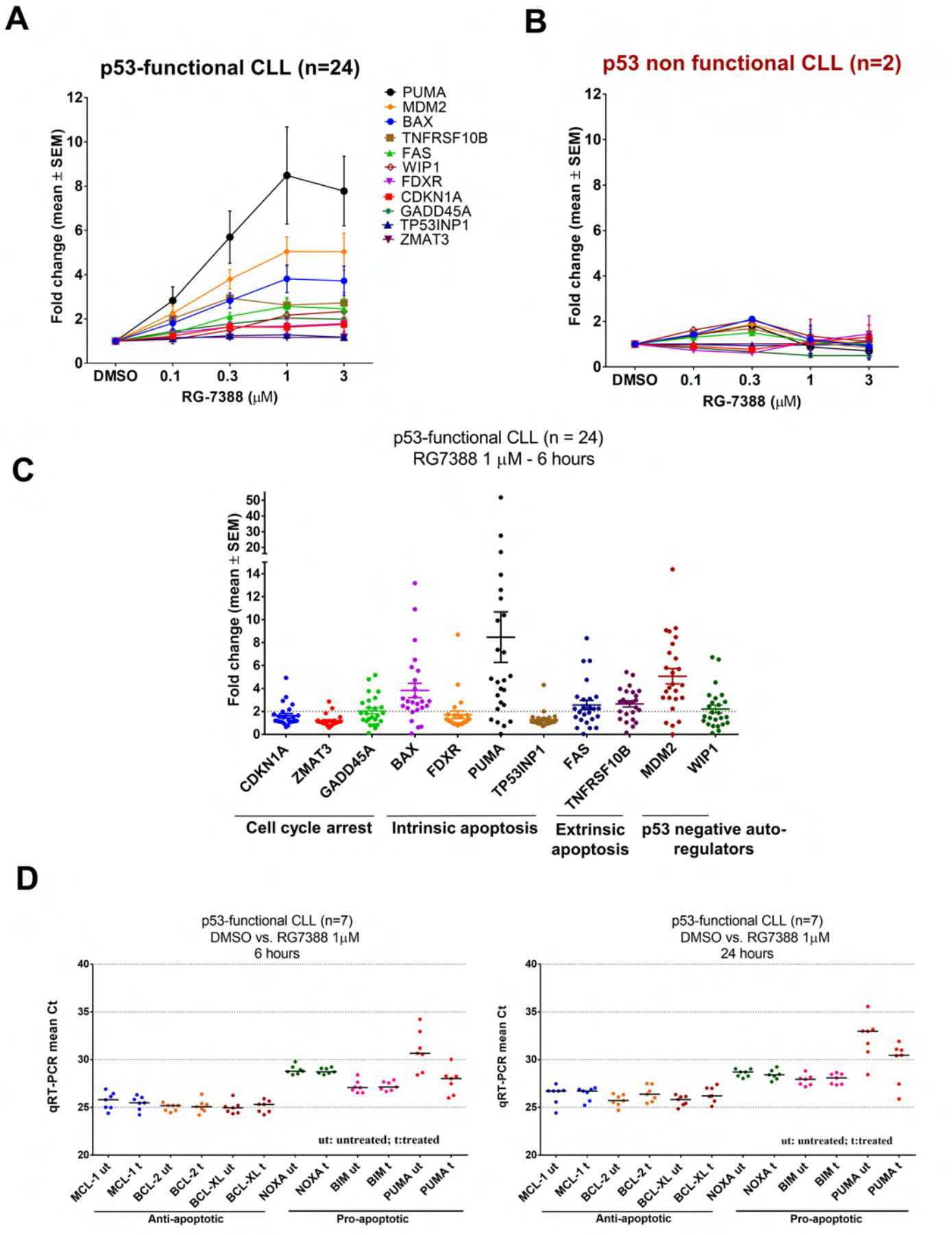
A
p53-functional CLL (n=24)
Fold change (mean ± SEM)
RG-7388 (μM)
DMSO
0.1
0.3
1
3
PUMA
MDM2
BAX
TNFRSF10B
FAS
WIP1
FDXR
CDKN1A
GADD45A
TP53INP1
ZMAT3
B
p53 non functional CLL (n=2)
C
p53-functional CLL (n = 24)
RG7388 1 μM - 6 hours
CDKN1A
ZMAT3
GADD45A
BAX
FDXR
PUMA
TP53INP1
FAS
TNFRSF10B
MDM2
WIP1
Cell cycle arrest
Intrinsic apoptosis
Extrinsic apoptosis
p53 negative auto-regulators
D
p53-functional CLL (n=7)
DMSO vs. RG7388 1μM
6 hours
qRT-PCR mean Ct
ut: untreated; t:treated
MCL-1 ut
MCL-1 t
BCL-2 ut
BCL-2 t
BCL-XL ut
BCL-XL t
NOXA ut
NOXA t
BIM ut
BIM t
PUMA ut
PUMA t
Anti-apoptotic
Pro-apoptotic
p53-functional CLL (n=7)
DMSO vs. RG7388 1μM
24 hours

Figure 3

A

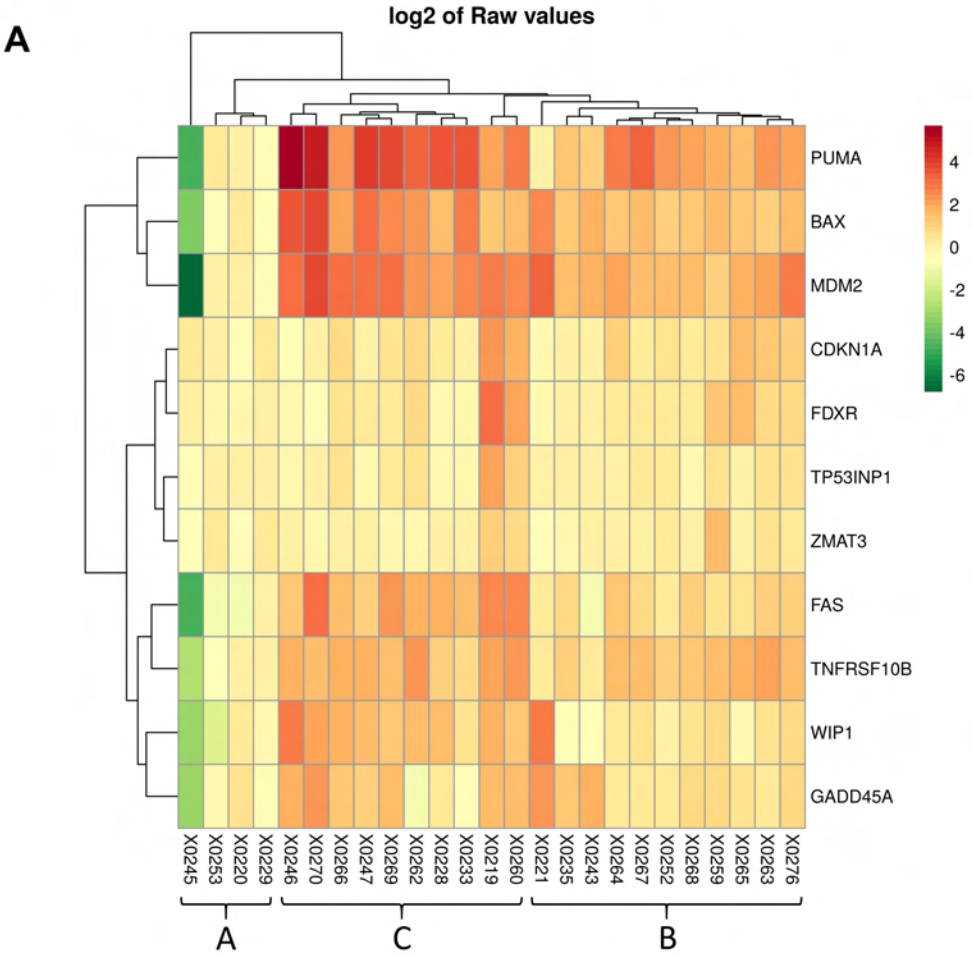

B

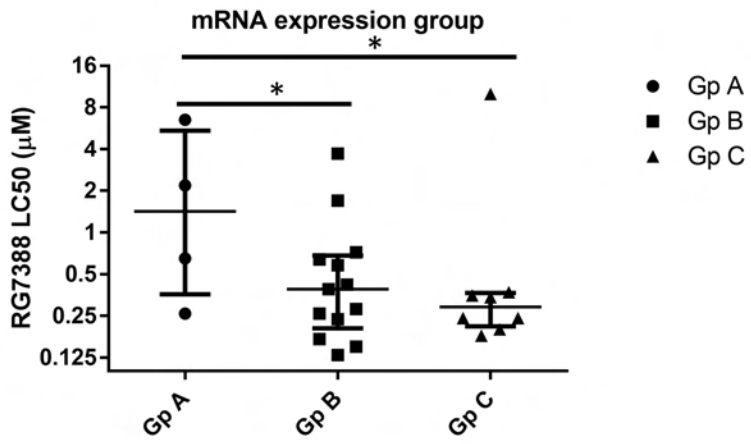

C

Holm-Sidak's multiple comparisons test	Mean Diff.	95% CI of diff	Significant?	Summary
Group A vs. Group B	1.92	0.24 to 3.61	Yes	*
Group A vs. Group C	2.12	0.29 to 3.95	Yes	*
Group B vs. Group C	0.19	-1.18 to 1.58	No	ns

Figure 4

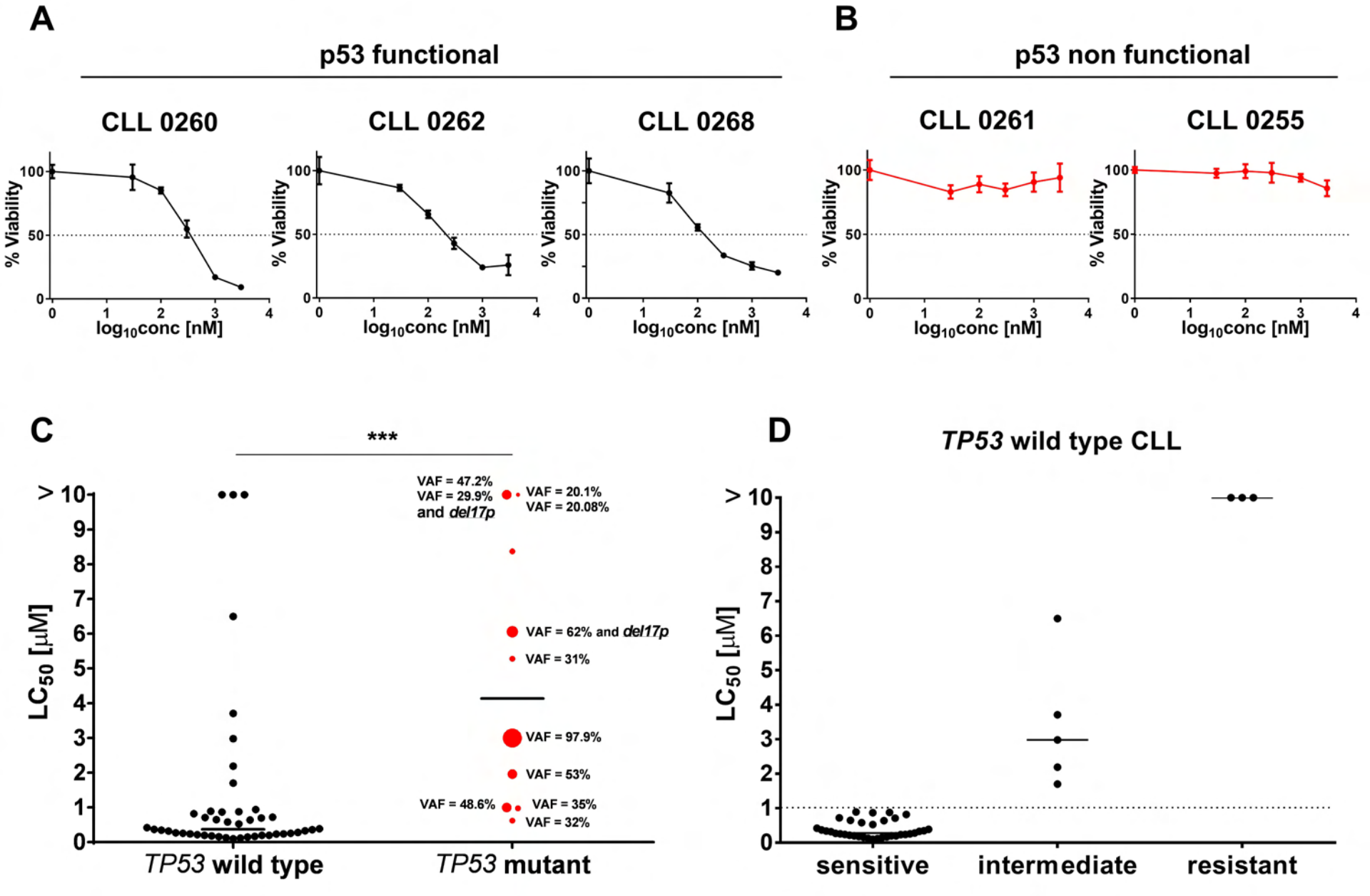

p-value according to Mann-Whitney test

Figure 5

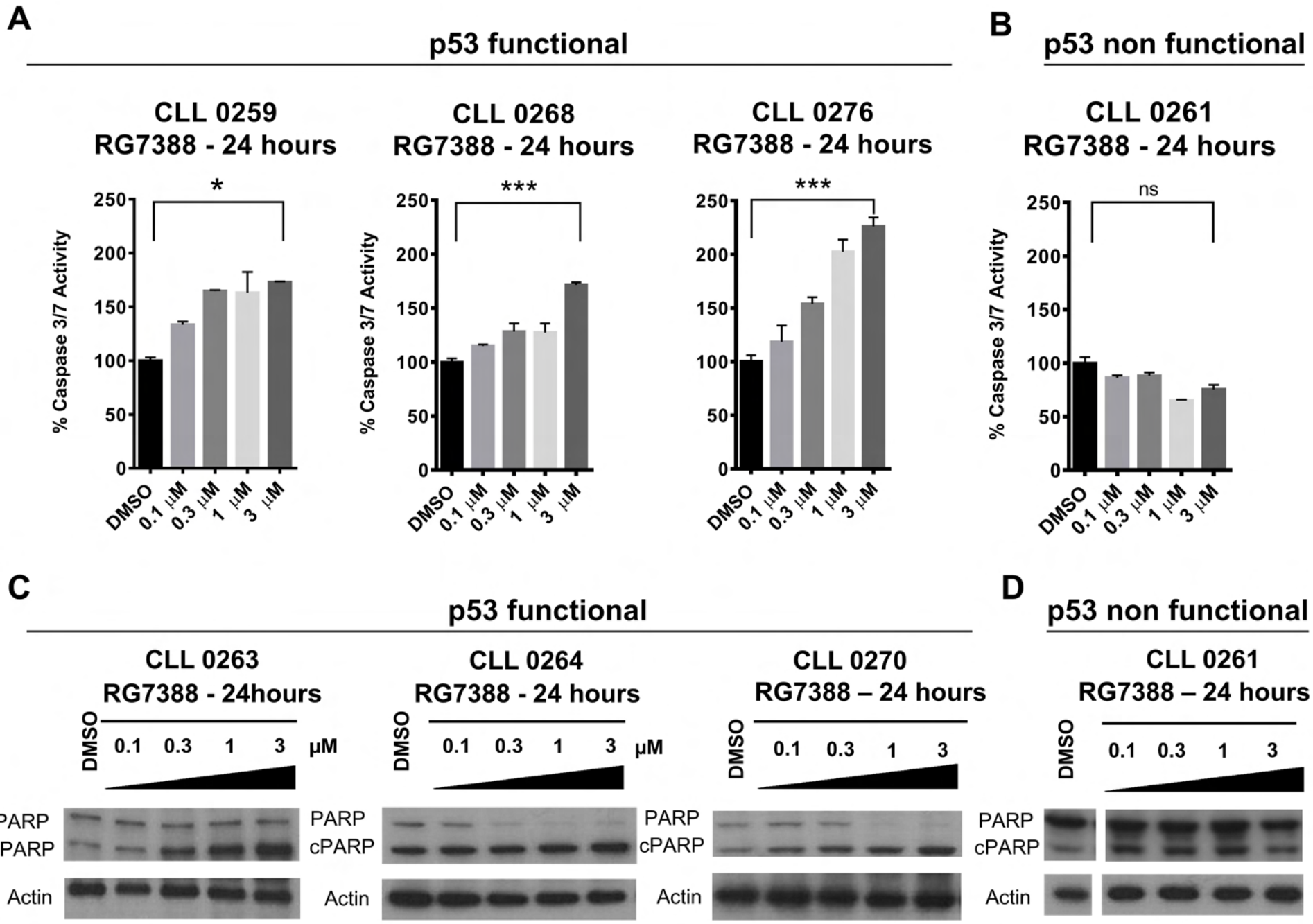
A
p53 functional
CLL 0259
RG7388 - 24 hours
CLL 0268
RG7388 - 24 hours
CLL 0276
RG7388 - 24 hours
% Caspase 3/7 Activity
*
***
***
DMSO
0.1 µM
0.3 µM
1 µM
3 µM
B
p53 non functional
CLL 0261
RG7388 - 24 hours
ns
C
p53 functional
CLL 0263
RG7388 - 24hours
CLL 0264
RG7388 - 24 hours
CLL 0270
RG7388 – 24 hours
DMSO
0.1 0.3 1 3 µM
PARP
cPARP
Actin
D
p53 non functional
CLL 0261
RG7388 – 24 hours

Figure 6

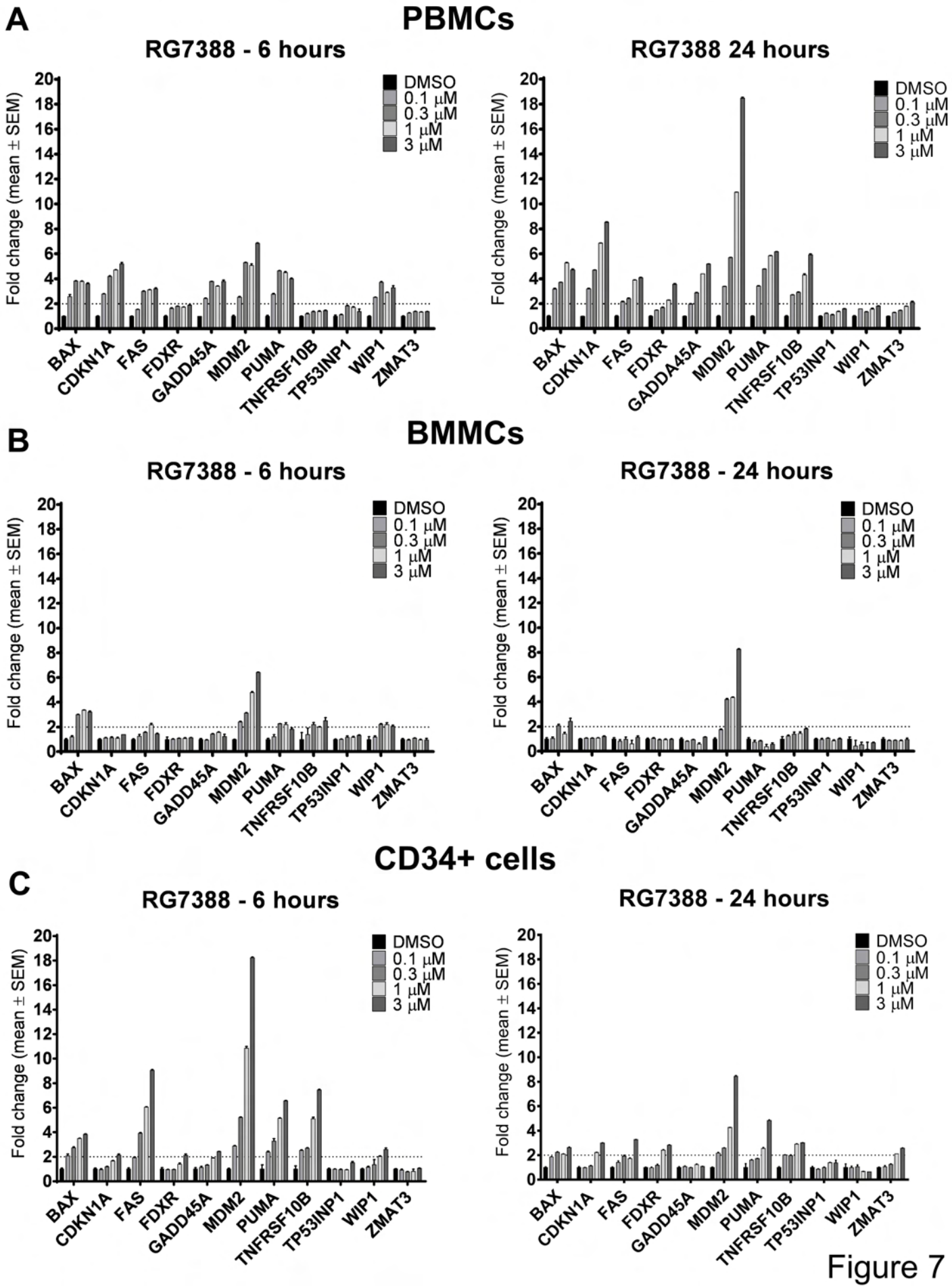
A
PBMCs
RG7388 - 6 hours
RG7388 24 hours
Fold change (mean ± SEM)
DMSO
0.1 μM
0.3 μM
1 μM
3 μM
BAX
CDKN1A
FAS
FDXR
GADD45A
MDM2
PUMA
TNFRSF10B
TP53INP1
WIP1
ZMAT3
B
BMMCs
RG7388 - 6 hours
RG7388 - 24 hours
C
CD34+ cells
RG7388 - 6 hours
RG7388 - 24 hours

Figure 7

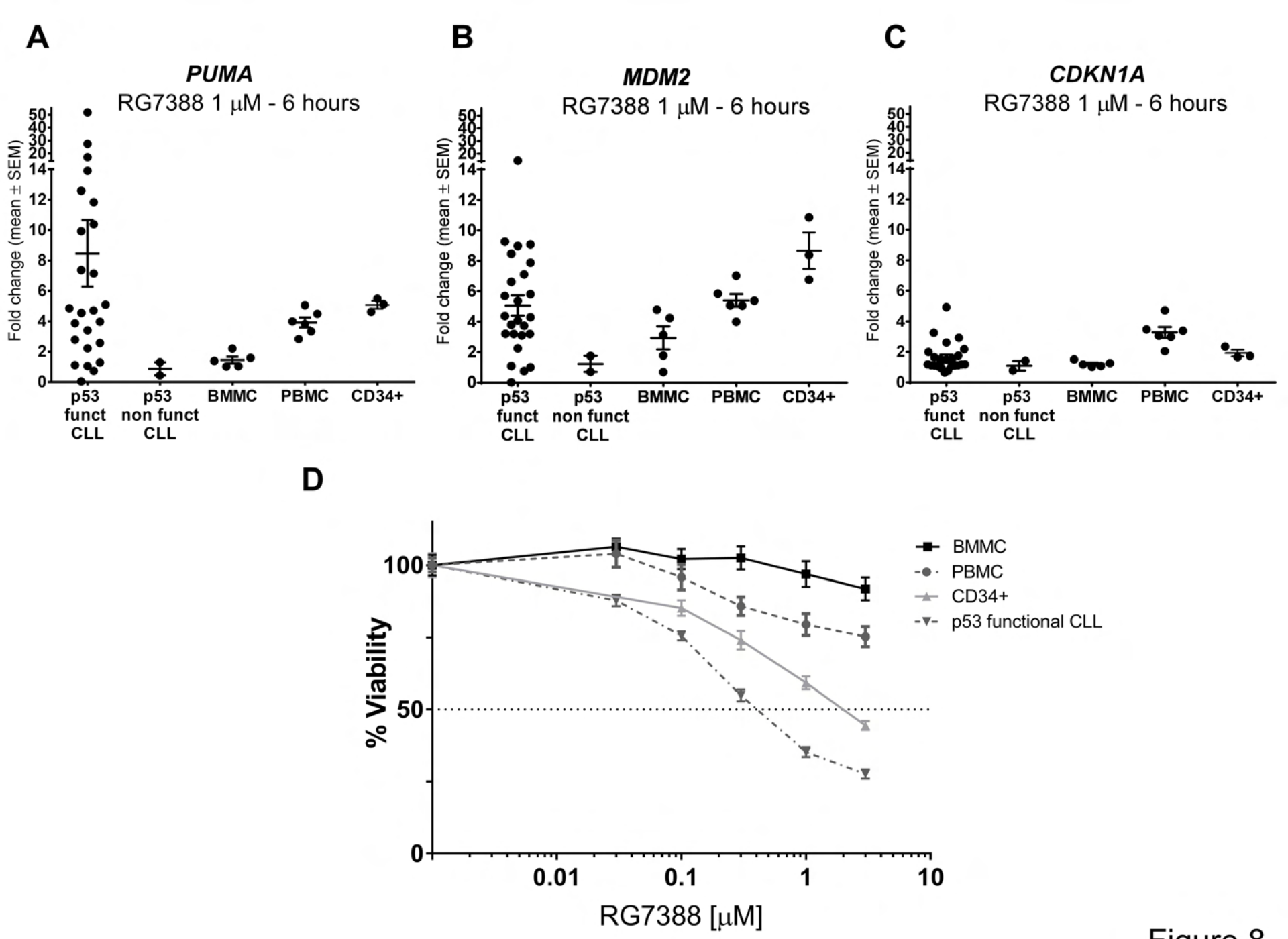
A
PUMA
RG7388 1 μM - 6 hours
Fold change (mean ± SEM)
p53 funct CLL
p53 non funct CLL
BMMC
PBMC
CD34+
B
MDM2
RG7388 1 μM - 6 hours
C
CDKN1A
RG7388 1 μM - 6 hours
D
% Viability
RG7388 [μM]
BMMC
PBMC
CD34+
p53 functional CLL

Figure 8

SUPPLEMENTARY APPENDIX

Non-genotoxic MDM2 inhibition selectively induces pro-apoptotic p53 gene signature in chronic lymphocytic leukemia cells

Carmela Ciardullo[1], Erhan Aptullahoglu[1], Laura Woodhouse[2], Wei-Yu Lin[1], Jonathan P Wallis[3], Helen Marr[3], Scott Marshall[4], Nick Bown[5], Elaine Willmore[1], John Lunec[1]

[1] Northern Institute for Cancer Research, Newcastle University, Newcastle upon Tyne, United Kingdom

[2] Faculty of Medical Sciences, Newcastle University, Newcastle upon Tyne, United Kingdom

[3] Department of Haematology, Freeman Hospital, The Newcastle upon Tyne NHS Foundation Trust, Newcastle upon Tyne, United Kingdom

[4] Department of Haematology, City Hospitals Sunderland NHS Trust, Sunderland, United Kingdom

[5] Northern Genetics Service, Institute of Genetic Medicine, Newcastle upon Tyne, United Kingdom

Supplementary Methods

Supplementary Figure Legends

SUPPLEMENTARY METHODS

Patients and cell isolation

CLL cells, normal peripheral blood mononuclear cells (PBMCs, n=6) and normal bone marrow mononuclear cells (BMMCs, n=5) were isolated by density gradient centrifugation (Lymphoprep, Axis-Shield) following the manufacturer's protocol. CLL cells and normal PBMCs were re-suspended at a density of 5.5 x 10^6 cells/ml in RPMI-1640 supplemented with 10% FCS, 2 mM glutamine, 1 mM sodium pyruvate, 1% penicillin/streptomycin and incubated at 37°C, 5% CO_2. BMMCs were re-suspended in Iscove's Modified Dulbecco's Medium (IMDM) supplemented with 20% FCS, 2 mM glutamine, 1 mM sodium pyruvate and 1% penicillin/streptomycin. CD34+ haematopoietic stem cells were isolated from BMMCs using a MACS immunomagnetic selection system (CD34 MicroBead Kit Ultra Pure, Miltenyi Biotec) and cultured for less than 7 days in StemMACS HSC Expansion Media XF supplemented with StemMACS HSC Expansion Cocktail (Miltenyi Biotec).

The purity of the isolated CD34+ hematopoietic progenitor cells was evaluated by flow cytometry. CD34+ cells and total BMMCs were stained using a fluorescent antibody (CD34-PE, clone: AC136, # 130-081-002, Miltenyi Biotec, UK) recognizing an epitope different from that recognized by the bead-bound CD34 monoclonal antibody QBEND/10. For optimal discrimination of CD34+ cells, cells were also counterstained with an antibody against CD45 (CD45‑FITC, # 130-080-202, Miltenyi Biotec, UK). Staining was carried out for 5 minutes at 4°C, cells were washed, resuspended in buffer and analysed at the Newcastle University Flow Cytometry Core Facility (FCCF) using a FACSCanto II (BD Biosciences).

Freshly isolated leukemic and normal cells were used immediately in all experiments and harvested at the indicated time points to asses viability, apoptosis, gene expression and for western blot analyses.

***Ex vivo* cytotoxicity assay**

5 x 10^5 CLL cells/well were seeded into a flat-bottom 96-well microtiter plate in triplicate and exposed to increasing concentrations of RG7388 for 48 hours. The final DMSO concentration (0.5%) was kept constant in each experiment.

Activated-XTT solution was prepared immediately before use by mixing XTT Reagent and the Activation Reagent in a 50:1 ratio. Cytotoxicity was evaluated by adding 50 µl of activated-XTT solution to 100 µl of drug-treated cells. Cells were then incubated for 8 hours at 37°C, 5% CO_2 and the microtiter plate was periodically assessed for the visual appearance of an orange color. After incubation, absorbance at 450nm was measured using a FluoStar Omega plate reader (BMG Labtech).

Western blot analysis

Thirty microgram aliquots of protein were electrophoresed on 4-20% denaturing SDS-polyacrylamide gradient gels (Bio-Rad, UK) and transferred onto nitrocellulose membrane (Amersham, UK). The samples were probed with antibodies against p53 (clone DO-7, Vector Laboratories), MDM2 (Calbiochem, OP46), p21 (Calbiochem, OP64), PARP (Trevigen, 4338-MC-50), PUMA (Calbiochem, PC686) and actin (Cell Signaling, 9284S). Peroxidase-conjugated anti-mouse (Dako, P0447) or anti-rabbit (Dako, P0448) secondary antibodies, ECL reagent (Amersham, UK) and blue light sensitive X-ray film (Fujifilm) were used for detection.

Apoptosis assay

5 x 10^5 CLL cells/well were seeded into a flat-bottom 96-well microtiter plate in triplicate and exposed to increasing concentrations of RG7388 for 24 hours. The final DMSO concentration (0.5%) was kept constant in each experiment.

Reconstituted Caspase-Glo 3/7 assay reagent (Promega, UK) was used for caspase detection in treated cells. The reagent provides a proluminescent caspase-3/7 substrate, which contains the tetrapeptide sequence DEVD, in combination with luciferase and a cell-lysing agent. The addition of the reconstituted Caspase-Glo 3/7 reagent directly to the assay well results in cell lysis, followed by caspase cleavage of the DEVD substrate, and the generation of luminescence. The amount of luminescence detected is proportional to the amount of caspase activity in the sample. Briefly, drug treated cells were mixed in a 1:1 ratio with reconstituted Caspase-Glo® 3/7 reagent and incubated for 30 minutes in the dark. Luminescence was measured with a FLUOstar Omega plate reader (BMG Labtech).

Co-culture and stimulation of CLL cells with CD40L-expressing cells

CD40L NIH-3T3 mouse fibroblasts were seeded into 24-well plates (3×10^5 cells/ml) in RPMI medium containing 10% heat-inactivated FCS, 2 mM L-glutamine and 1% penicillin/streptomycin and allowed to adhere. The cells were irradiated (35 Gy) to prevent proliferation and incubated at 37°C, 5% CO_2 overnight. CLL cells were thawed and resuspended at a density of 2×10^7 cells/mL in RPMI supplemented with 10% FCS, glutamine, 1% penicillin/streptomycin and 10 ng/mL human IL4. Cells were then seeded onto the CD40L monolayer at a density of 1×10^7 per well and incubated at 37°C, 5% CO_2. Cells were monitored daily and began to proliferate after approximately 96 hours.

After 96 hours, CLL cells were counted as a pre-treatment control and exposed to increasing concentrations of RG7388. Cells were counted at 24 hour intervals thereafter. At 6 and 24 hour intervals after drug exposure, cells were harvested for western immunoblot and qRT-PCR mRNA expression profiling. Growth inhibitory and cytotoxic response to drug was measured after 48 hours drug exposure. Cell counts were performed using a Coulter Counter (Beckman Coulter, High Wycombe, UK) with the threshold set at 5-12 μm. Counts were plotted against

time and as a concentration-dependent response curve generated from the cell counts at the terminal 48hr exposure period expressed as a % of the vehicle control. Throughout the experiment, CLL cells were re-seeded onto a fresh CD40L feeder layer every 72 hours and drug-containing medium was replenished with fresh medium containing the same concentration of RG7388 every 48 hours.

Cell cycle analysis of CD34+ haematopoietic stem cells

Positively-selected CD34+ cells were incubated with RG7388 for 24 hours. Cells were washed with PBS and fixed with cold 70% ethanol for 30 minutes on ice. Cells were then resuspended in 500 μL PBS with 100 μg/mL propidium iodide (Sigma) and 200 μg/mL RNAse A (Sigma). Samples were analyzed on a FACSCaliburTM flow cytometer using CellQuest Pro software (Becton Dickinson, Oxford, UK). Cell cycle distribution was determined using Cyflogic software (CyFlo Ltd, Turku, Finland).

SUPPLEMENTARY FIGURE LEGENDS

Figure S1

PUMA protein expression following treatment with RG7388 and time dependent loss of viability

(A) Western blot analysis showing representative examples of dose dependent PUMA protein induction by *ex vivo* treatment of CLL samples with RG7388 for 24hours (CLL265 and CLL268). Two examples of non-functional p53 stabilisation with minimal downstream PUMA expression are included (CLL281 and CLL297) together with one example of high basal PUMA expression which is further increased by RG7388 (CLL 302). (B) RG7388 dose and exposure time dependent loss of viability measured by XTT assay for two representative wild-type p53 CLL patient samples exposed to a concentration range of 0.1-10μM RG7388 for 12, 24 and 48hrs. Results are expressed as % relative to DMSO vehicle control, presented as mean ± standard error of mean (SEM) for three intra-experimental repeats.

Figure S2

CLL sample with subclonal 17p deletion treated with RG7388 shows functional activation of p53, upregulation of pro-apoptotic p53-targets and cytotoxicity

(A) Western immunoblot of a CLL sample (CLL 0269) harbouring a subclonal (22%) 17p deletion treated with RG7388 for 6 and 24 hours. Sample shows stabilisation of p53 and induction of MDM2, p21 and cleaved PARP. (B) qRT-PCR results for CLL 0269 treated with RG7388 for 6 and 24 hours showing fold-change of mRNA for p53-target genes and in particular preferential induction of *PUMA.* Data are presented as mean ± standard error of mean (SEM) of three repeats (C) Increase in Caspase 3/7 activity in CLL 0269 exposed to RG7388 for 24 hours. Data are presented as mean ± standard error of mean (SEM) for three repeats (D) Response of CLL 0269 exposed to increasing concentrations of RG7388 for 48

hours. Concentration-dependent decrease in cell viability assessed by XTT assay indicates sensitivity to RG7388. Data are presented as mean ± standard error of mean (SEM) for three repeats.

Figure S3

RG7388 induces cytotoxicity in cells isolated from CLL patients for the *TP53* wild-type subset, regardless of disease stage, *IGHV* status and other cytogenetics abnormalities.

(A) RG7388 LC_{50} values for CLL samples from patients with Binet A, B or C stage of disease. (B) RG7388 LC_{50} values for CLL samples from patients with mutated or unmutated *IGHV* genes.

(C) RG7388 LC_{50} values for CLL samples from patients with trisomy of chromosome 12 (+12), deletion of chromosome 13q, deletion of chromosome 11q and no cytogenetics abnormalities. Horizontal bars represent the median. The p-values were calculated by Mann–Whitney test.

Figure S4

RG7388 inhibits CLL proliferation induced by microenvironment stimuli

(A) CLL cells from patient 0260 were cultured on CD40L-expressing feeder cells for 96 hours followed by treatment with increasing concentrations of RG7388 at the start of proliferation. Cells were counted at 24 hour intervals for a further 96 hours. (B) (C) Concentration-dependent reduction in CLL cell numbers after 48 hours of RG7388 exposure compared with untreated controls (CLL sample 0260, CLL sample 0278). (D) (E) Western immunoblots blot of a p53-functional CLL sample (CLL 0278) unstimulated or stimulated with CD40L/IL4 and then treated with RG7388 for 6 and 24 hours. Stimulated sample shows a greater stabilisation of p53 and induction of MDM2 and p21 but no cleaved PARP compared to the unstimulated counterpart. (F) qRT-PCR results for fold-change of *PUMA*, *MDM2* and *CDKN1A* mRNA

measured following 6 and 24 hours exposure to RG7388 in CLL 0278 cells which were left unstimulated or stimulated with CD40L/IL4.

Figure S5

Caspase 3/7 activation is triggered by RG7388 selectively in CLL cells but not in normal PBMC or BMMC cells.

Caspase 3/7 activity for n=9 p53-functional CLL samples, n=1 p53-non-functional CLL sample, n=3 normal BMMC samples and n=6 normal PBMC samples exposed to 1 μM RG7388 for 24 hours. Caspase 3/7 activity is represented as % change relative to DMSO solvent control. Data are presented as mean ± standard error of mean (SEM). p-value is calculated by Mann–Whitney test.

Figure S6

MDM2 inhibition by RG7388 induces cell cycle distribution changes in positively-selected CD34+ haematopoietic stem cells

(A) FACS plots showing CD34+ cells (left) sorted to high purity by antibody-based magnetic bead cell separation (MACS) from mononuclear cells isolated from human bone marrow (right). Flow cytometry of enriched CD34+ cells (left) shows that of the live cells, >80% express CD34, of which 39% co-express CD45. (B) FACS histograms showing CD34+ expression in mononuclear cells isolated from human bone marrow (left) and haematopoietic CD34+ cells purified by MACS selection (right). (C) Cell cycle distribution analysis of CD34+ cells incubated with RG7388 for 24 hours showing an increased proportion of cells in G0/G1 phase and a reduction of cells in S phase. (D) Bar-chart showing a slight increase of Sub-G1 events in CD34+ cells exposed to RG7388 for 24 hours.

Figure S7

***MDM2* and *PUMA* basal expression levels vary across CLL samples but do not predict response to RG7388 in the *TP53* wild-type subset**

(A) Basal *MDM2* expression levels expressed as Ct values measured by qRT-PCR in CLL samples, normal BMMCs, normal PBMCs and normal CD34+ cells. The median *MDM2* basal levels in CLL samples was statistically different to that of PBMCs. Ct values are expressed as mean of at least three repeats. P-values are calculated by Mann-Whitney test. (B) Basal *PUMA* expression levels expressed as Ct values and measured by qRT-PCR in CLL samples, normal BMMCs, normal PBMCs and normal CD34+ cells. The median *PUMA* basal levels in CLL samples was not different to that of normal cells. Ct values are expressed as mean of at least three repeat. p-values are calculated by Mann-Whitney test. (C) *MDM2* mRNA expression levels expressed as Ct values and measured by qRT-PCR in CLL samples grouped according to different cytotoxic responses to RG7388. The distribution of *MDM2* basal levels in CLL samples showing sensitivity to RG7388 (LC_{50}<1μM) was not statistically significantly different to that of samples showing intermediate response/resistance (LC_{50}>1μM) to RG7388. Ct values are expressed as mean of at least three repeats. P-values were calculated by Mann-Whitney test. (D) *PUMA* mRNA levels expressed as Ct values and measured by qRT-PCR in CLL samples showing different cytotoxic responses to RG7388. The distribution of *PUMA* basal levels in CLL samples showing sensitivity to RG7388 (LC_{50}<1μM) was not statistically significantly different to that of samples showing intermediate response/resistance (LC_{50}>1μM) to RG7388. Ct values are expressed as mean of at least three repeats. P-values were calculated by Mann-Whitney test. (E) (F) Comparison between (E) *MDM2* and (F) *PUMA* basal Ct values and RG7388 LC_{50} concentrations for CLL samples. The r-value indicates Pearson's correlation coefficient with associated p-value indicating no significant correlation.

Figure S8

***MDM2* and *PUMA* fold inductions by RG7388 are alone not biomarkers of drug-induced cytotoxicity for the subset of wild-type p53 CLL cases**

(A) (B) Correlation of (A) *MDM2* and (B) *PUMA* mRNA fold induction (exposure 1 µM RG7388 for 6 hours) and RG7388 LC_{50} concentrations of CLL samples. The r-value is Pearson's correlation coefficient and associated p-values indicate there is no significant correlation.

Figure S9

Combination treatments of CLL cells *ex vivo* with RG7388 and either venetoclax (ABT199) or Ibrutinib

(A) (B) Combination treatment with RG7388 and ABT199 compared with either agent alone showing a significant additive effect on cell killing. Drug exposure was 48hours and viability measured by XTT assay. (C) (D) Combination treatment with RG7388 and Ibrutinib showing no additional effect of Ibrutinib over that seen with RG7388 alone.

Table S1. Characteristics of the CLL cohort

Tumour ID	Age	Binet Stage	IgVH	Cytogenetics	*TP53* status (NGS)	*TP53* mutation	RG7388 LC_{50} (µM)
212	57	C	U	12+	WT		0.7
216	81	A	M	del13q	WT		0.36
217	66	C	U	del11q	MUT	c.524G>A, p.R175H	1.96
218	84	A	M	none	WT		0.22
219	86		U	del13q	WT		0.26
220	57	A	M	del13q	WT		0.26
221	86	C	M	none	WT		0.17
222	76	C	M	del11q, del13q, 12+	WT		0.82
224	69	C	M	bi13q	MUT	c.578A>T, p.H193L	5.28
225	66		M	none	WT		0.2
226	58	A	M	none	WT		0.32
227	71	A	M	bi13q	WT		0.89
228	79	B	U	12+	WT		0.18
229	67	B	M	del13q	WT		6.5
230	79	B	U	12+	WT		0.16
231	60	A	M	none	WT		0.87
233	66	C	U	del11q, del13q	WT		>10
234	81	B	U	del11q, del13q	WT		0.27
235	77	A	M	bi13q	WT		3.71
237	77	B	U	del17p	MUT	c.701A>G, p.Y234C	6.06
239	56		M	del13q	WT		0.1
240	72		U	none	WT		>10
241	80	A	M	none	WT		>10
242	78	C	M	none	WT		0.2

243	76	A	M	none	WT		0.72
244	72		M	del13q	MUT	c.832C>T, p.P278S	0.62
245	79	A	U	del13q	WT		2.19
246	76	C		none	WT		0.24
247	83	A		none	WT		0.2
248	67	A	M	del13q	MUT	c.850A>T, p.T284S	>1
249	66	C		del13q	WT		2.98
250	85	B	M	del13q	WT		0.71
251	64	B	M	del17p, del13q	MUT	c.742C>T, p.R248W; c.673-2A>C	>10
252	68	C		del13q	WT		0.13
253	61		M	del13q	WT		0.65
254	72	Apro		del11q, del13q	WT		0.53
255	80			NA	NA		8.37
257	72	A		del13q, del 11q	WT		0.12
258	72			del13q, del11q	MUT	c.626_627delGA, p.R209fs*6	0.98
259	88		U	del13q	WT		0.58
260	89			del13q	WT		0.39
261	79	C	M	del13q	MUT	c.626_627delGA, p.R209fs*6	>3
262	72	A		none	WT		0.24
263	80	A		none	WT		0.64
264	71			del11q	WT		0.42
265	86			del13q, del11q	WT		0.28
266	59			del13q	WT		0.37
267	60	A	M	del13q	WT		0.24
268	83	A	M	del13q	WT		0.15

269	63			del17p	WT		0.34
270	75			del13q	WT		0.35
272	69		M	none	WT		0.33
273	61		U	none	MUT	c.1067G>C, p.G356A; c.1069A>C, p.K357Q	>10
275	88		M	none	WT		0.88
276	67	C		none	WT		1.7

Table S2. Primers used for qRT-PCR			
Gene Symbol	**Gene name**	Primer Forward (5'-3')	Primer Reverse (5'-3')
GAPDH	Glyceraldehyde 3-phosphate dehydrogenase	CGACCACTTTGTCAAGCTCA	GGGTCTTACTCCTTGGAGGC
CDKN1A	Cyclin Dependent Kinase Inhibitor 1A	TGTCCGTCAGAACCCATGC	AAAGTCGAAGTTCCATCGCTC
MDM2	Mouse double minute 2 homolog	AGTAGCAGTGAATCTACAGGGA	CTGATCCAACCAATCACCTGAAT
PUMA (BBC3)	p53 upregulated modulator of apoptosis	ACCTCAACGCACAGTACGA	CTGGGTAAGGGCAGGAGTC
BAX	BCL2 Associated X	CCCGAGAGGTCTTTTTCCGAG	CCAGCCCATGATGGTTCTGAT
FAS	Fas cell surface death receptor	AGATTGTGTGATGAAGGACATGG	TGTTGCTGGTGAGTGTGCATT
FDXR	Ferredoxin reductase	CAGCATTGGGTATAAGAGCCG	GGCCTGGCACATCCATAACC
TNFRSF10B	Tumor necrosis factor receptor superfamily, member 10b	ATGGAACAACGGGGACAGAAC	CTGCTGGGGAGCTAGGTCT
TP53INP1	Tumor protein p53 inducible nuclear protein 1	TCTTGAGTGCTTGGCTGATACA	GGTGGGGTGATAAACCAGCTC
ZMAT3	Zinc finger matrin-type 3	CCTTACTTCAATCCCCGCTCT	CTTCGCCAGCTCCAACATTAC
GADD45A	Growth arrest and DNA damage inducible alpha	GAGAGCAGAAGACCGAAAGGA	CAGTGATCGTGCGCTGACT
WIP1 (PPM1D)	Protein phosphatase, Mg2+/Mn2+ dependent 1D	TTTCTCGCTTGTCACCTTGC	TTCCAAGAACCACCCCTGAG
BCL2	Protein phosphatase 1, regulatory subunit 50	GGTGGGGTCATGTGTGTGG	CGGTTCAGGTACTCAGTCATCC
MCL1	MCL1 apoptosis regulator, BCL2 family member	GTGCCTTTGTGGCTAAACACT	AGTCCCGTTTTGTCCTTACGA
BCL2L1 (BCL-XL)	BCL2 Like 1	QIAGEN QUANTITECT PRIMER ASSAY QT00236712	
PMAIP1 (NOXA)	Phorbol-12-myristate-13-acetate-induced protein 1	TGCTACACAATGTGGCGTC	ACTTGGACATGGCCTCCCTTA
BCL2L11 (BIM)	BCL2-Like 11	TAAGTTCTGAGTGTGACCGAGA	GCTCTGTCTGTAGGGAGGTAGG

A

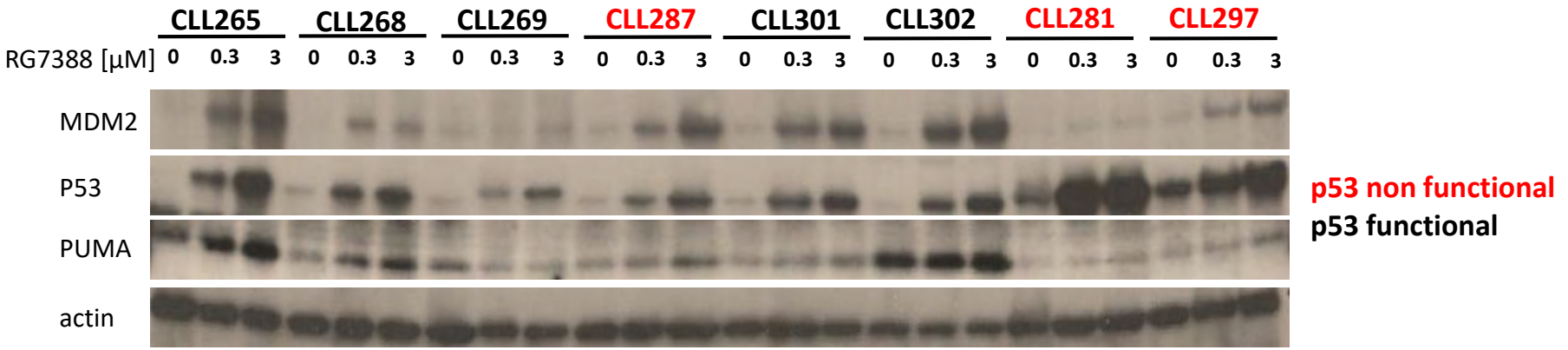
CLL265
CLL268
CLL269
CLL287
CLL301
CLL302
CLL281
CLL297
RG7388 [µM] 0 0.3 3 0 0.3 3 0 0.3 3 0 0.3 3 0 0.3 3 0 0.3 3 0 0.3 3 0 0.3 3
MDM2
P53
PUMA
actin
p53 non functional
p53 functional

B

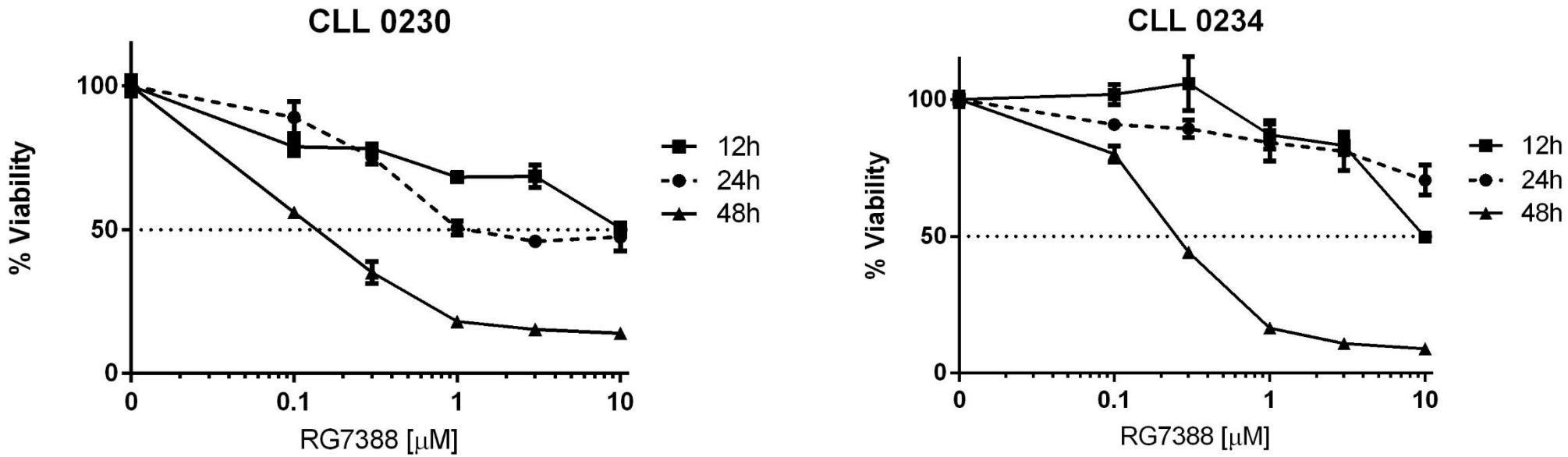
CLL 0230
% Viability
100
50
0
0
0.1
1
10
RG7388 [µM]
12h
24h
48h
CLL 0234
% Viability
100
50
0
0
0.1
1
10
RG7388 [µM]
12h
24h
48h

Figure S1

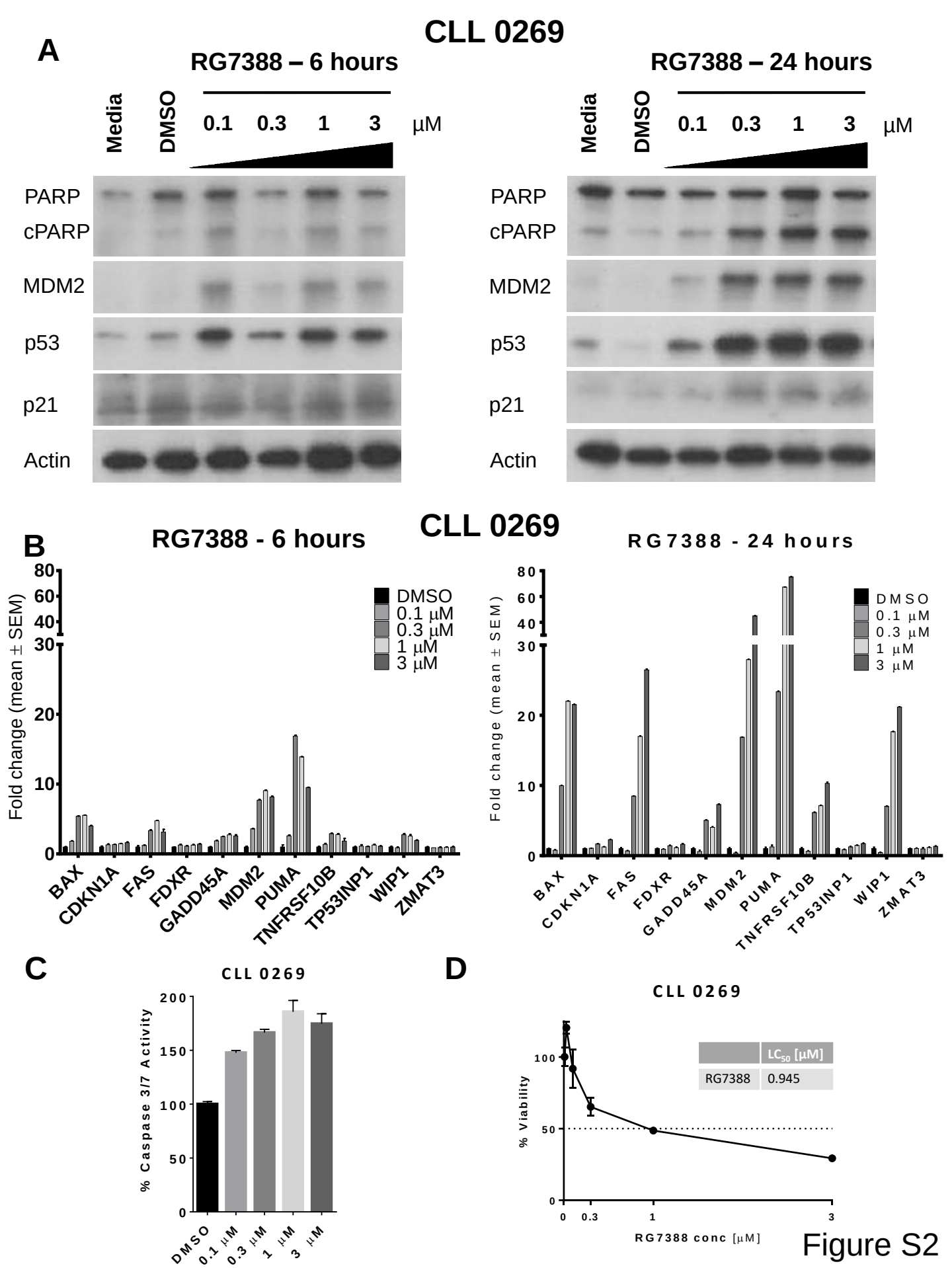
CLL 0269
A
RG7388 – 6 hours
RG7388 – 24 hours
Media
DMSO
0.1
0.3
1
3
µM
PARP
cPARP
MDM2
p53
p21
Actin
CLL 0269
B
RG7388 - 6 hours
RG7388 - 24 hours
Fold change (mean ± SEM)
DMSO
0.1 µM
0.3 µM
1 µM
3 µM
BAX
CDKN1A
FAS
FDXR
GADD45A
MDM2
PUMA
TNFRSF10B
TP53INP1
WIP1
ZMAT3
C
CLL 0269
% Caspase 3/7 Activity
DMSO
0.1 µM
0.3 µM
1 µM
3 µM
D
CLL 0269
% Viability
LC50 [µM]
RG7388
0.945
RG7388 conc [µM]

Figure S2

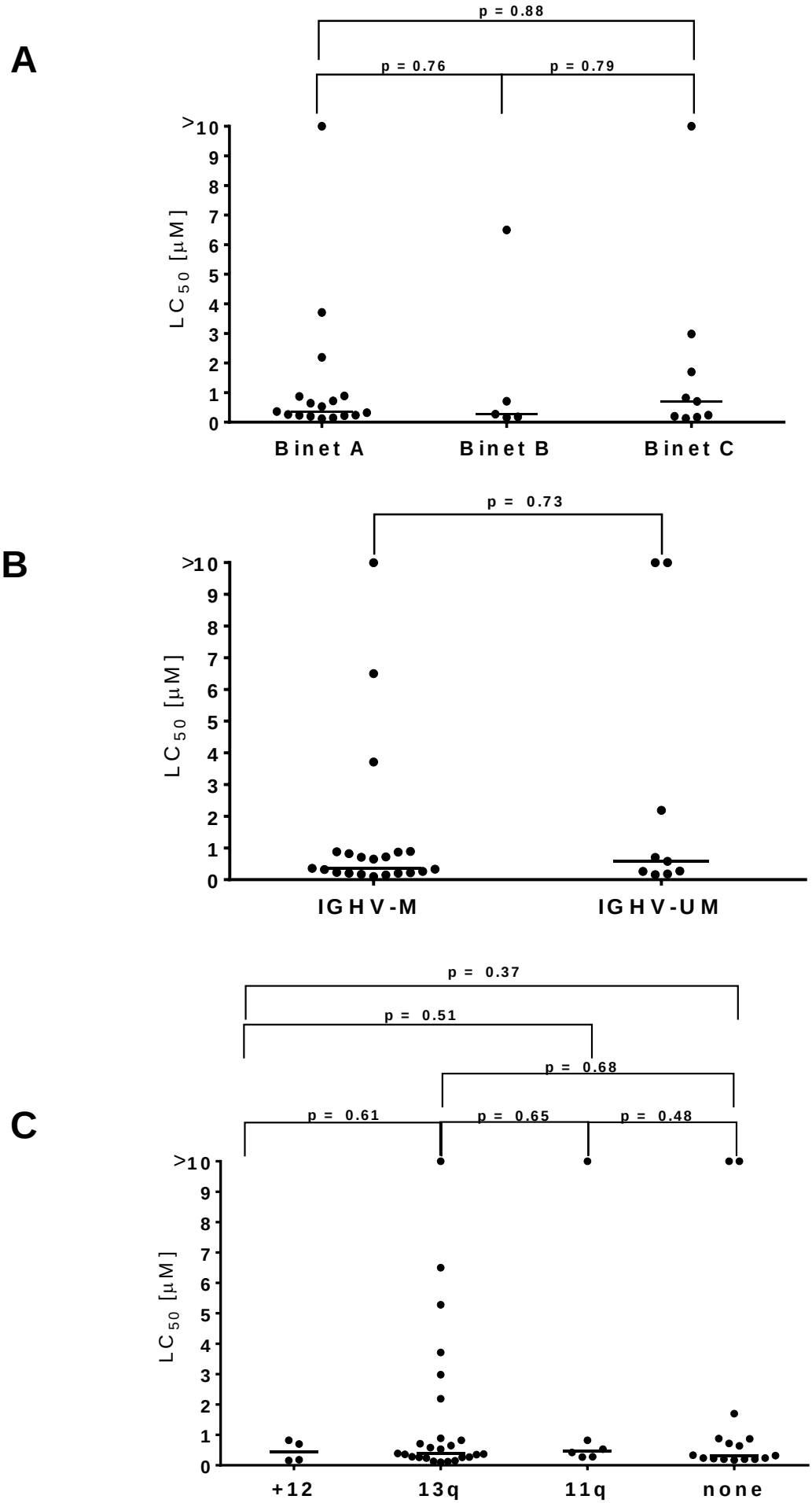
A
p = 0.88
p = 0.76
p = 0.79
LC50 [µM]
>10
9
8
7
6
5
4
3
2
1
0
Binet A
Binet B
Binet C
B
p = 0.73
LC50 [µM]
>10
9
8
7
6
5
4
3
2
1
0
IGHV-M
IGHV-UM
C
p = 0.37
p = 0.51
p = 0.68
p = 0.61
p = 0.65
p = 0.48
LC50 [µM]
>10
9
8
7
6
5
4
3
2
1
0
+12
13q
11q
none

Figure S3

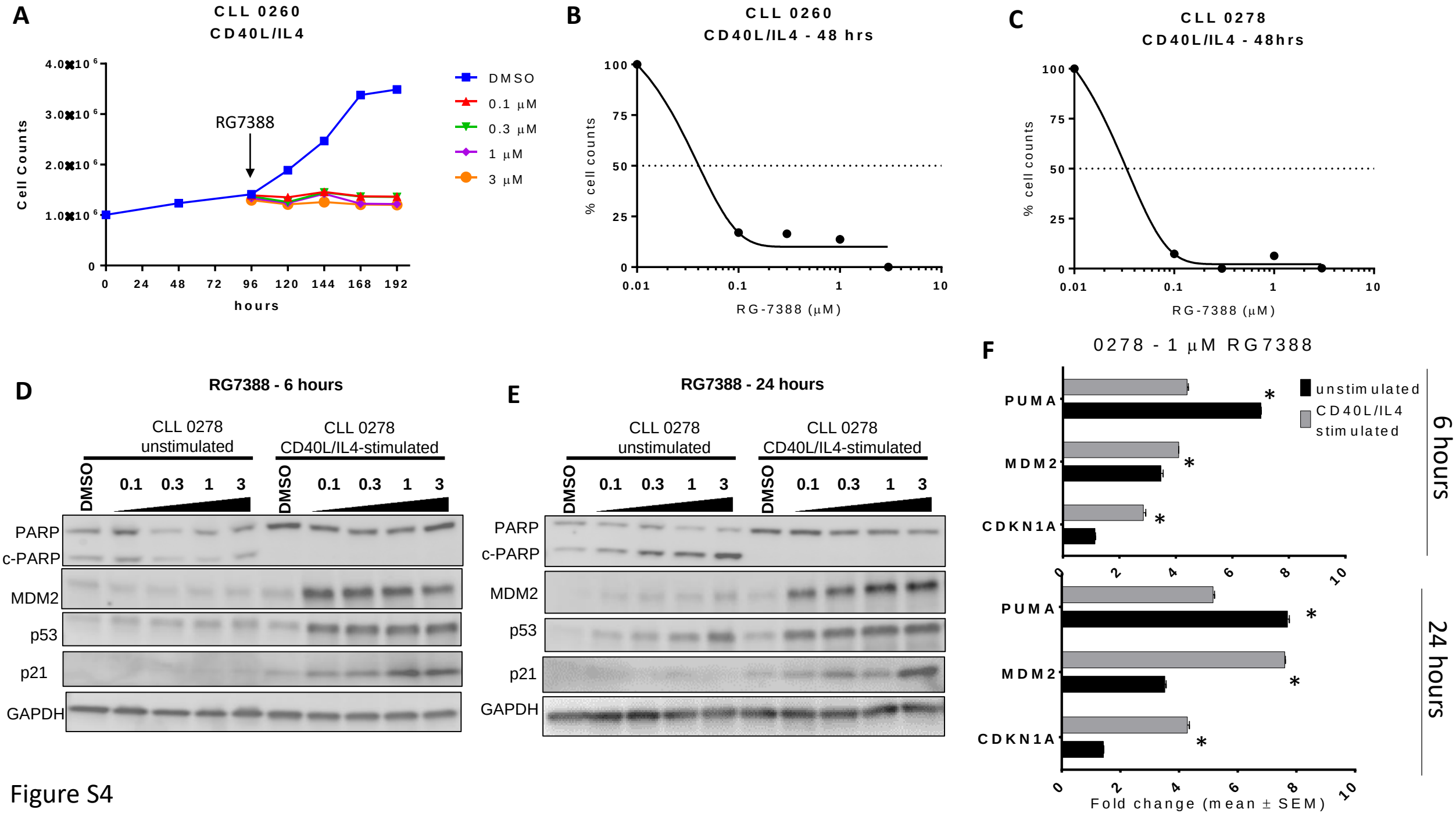
A
CLL 0260
CD40L/IL4
Cell Counts
hours
RG7388
DMSO
0.1 µM
0.3 µM
1 µM
3 µM
B
CLL 0260
CD40L/IL4 - 48 hrs
% cell counts
RG-7388 (µM)
C
CLL 0278
CD40L/IL4 - 48hrs
% cell counts
RG-7388 (µM)
D
RG7388 - 6 hours
CLL 0278 unstimulated
CLL 0278 CD40L/IL4-stimulated
DMSO
0.1
0.3
1
3
PARP
c-PARP
MDM2
p53
p21
GAPDH
E
RG7388 - 24 hours
CLL 0278 unstimulated
CLL 0278 CD40L/IL4-stimulated
F
0278 - 1 µM RG7388
unstimulated
CD40L/IL4 stimulated
PUMA
MDM2
CDKN1A
6 hours
24 hours
Fold change (mean ± SEM)

Figure S4

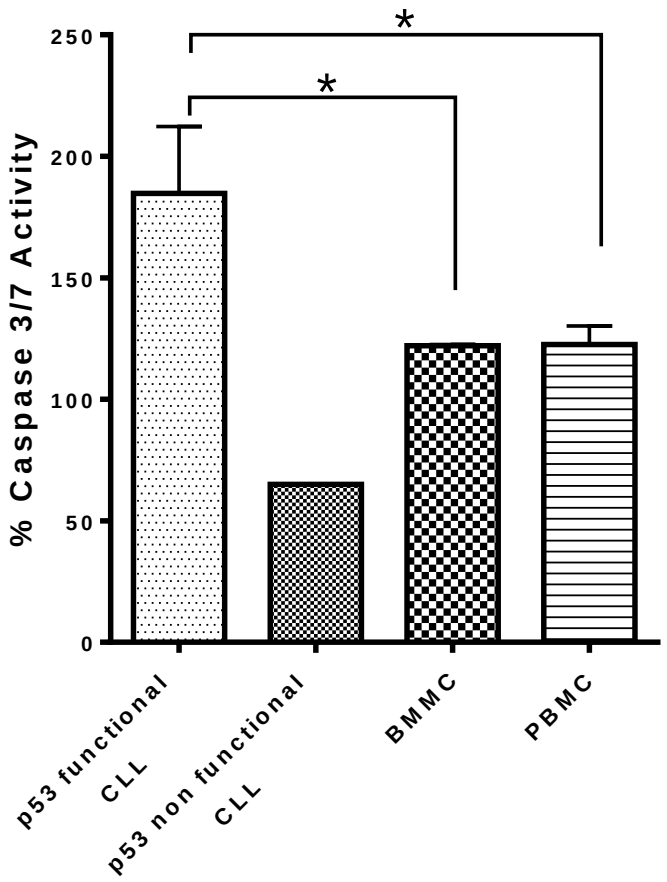
RG7388 - 1 μM - 24 hours
% Caspase 3/7 Activity
250
200
150
100
50
0
*
*
p53 functional CLL
p53 non functional CLL
BMMC
PBMC

Figure S5

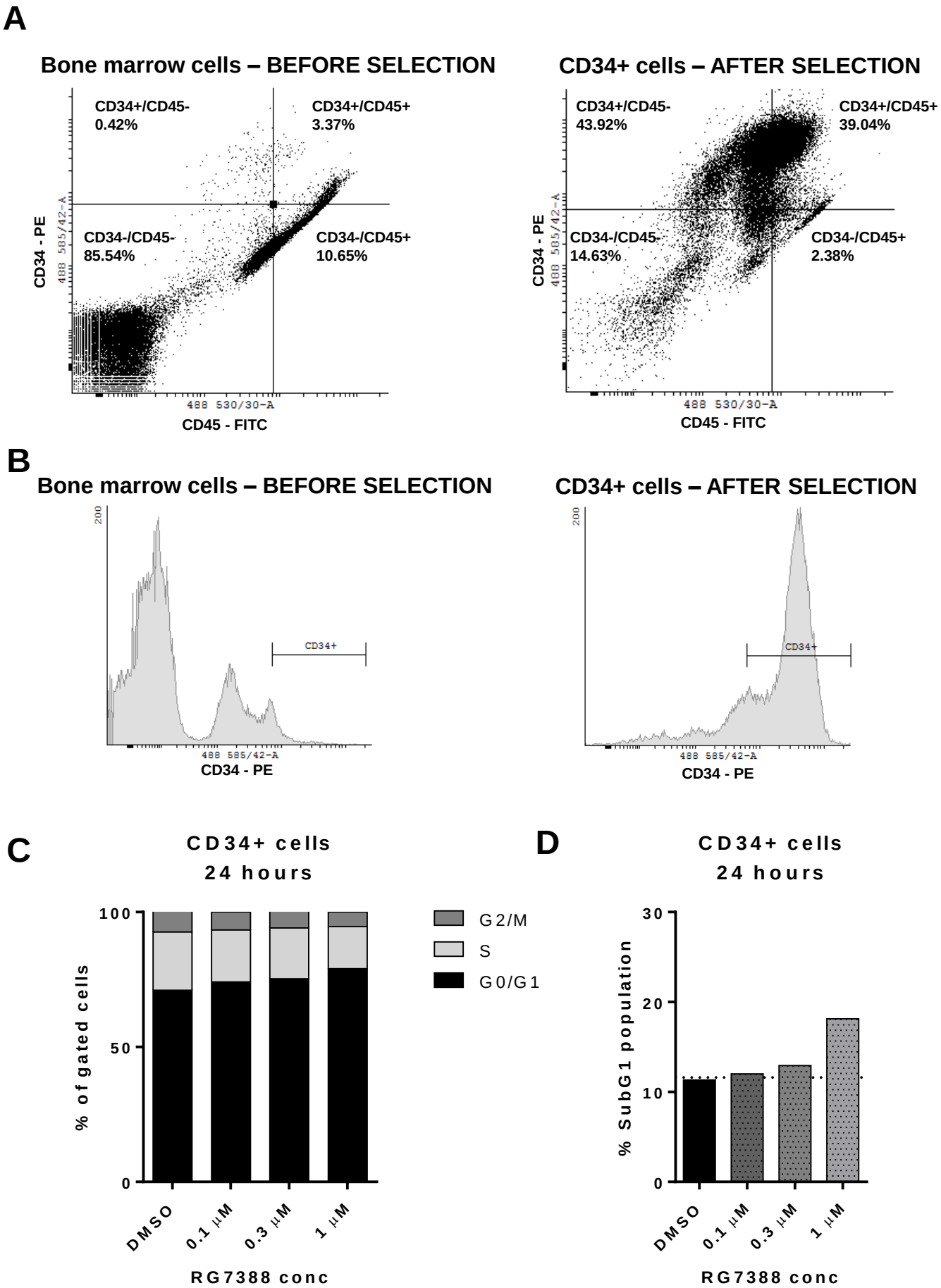
A
Bone marrow cells – BEFORE SELECTION
CD34+/CD45-
0.42%
CD34+/CD45+
3.37%
CD34-/CD45-
85.54%
CD34-/CD45+
10.65%
CD34 - PE
488 585/42-A
488 530/30-A
CD45 - FITC
CD34+ cells – AFTER SELECTION
CD34+/CD45-
43.92%
CD34+/CD45+
39.04%
CD34-/CD45-
14.63%
CD34-/CD45+
2.38%
CD34 - PE
488 585/42-A
488 530/30-A
CD45 - FITC
B
Bone marrow cells – BEFORE SELECTION
200
CD34+
488 585/42-A
CD34 - PE
CD34+ cells – AFTER SELECTION
200
CD34+
488 585/42-A
CD34 - PE
C
CD34+ cells
24 hours
100
50
0
% of gated cells
G2/M
S
G0/G1
DMSO
0.1 µM
0.3 µM
1 µM
RG7388 conc
D
CD34+ cells
24 hours
30
20
10
0
% SubG1 population
DMSO
0.1 µM
0.3 µM
1 µM
RG7388 conc

Figure S6

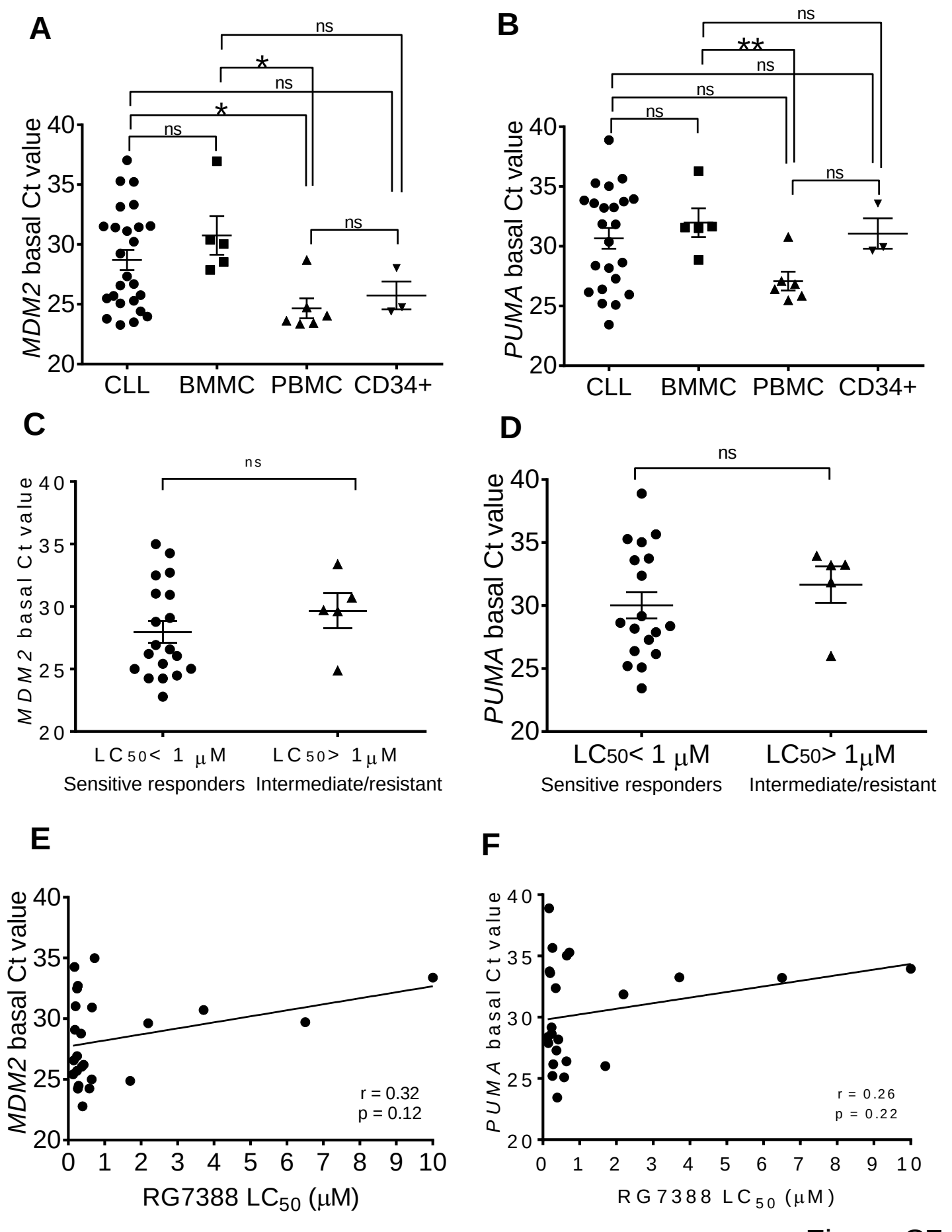
A
ns
*
ns
*
ns
ns
MDM2 basal Ct value
40
35
30
25
20
CLL
BMMC
PBMC
CD34+
B
ns
**
ns
ns
ns
ns
PUMA basal Ct value
40
35
30
25
20
CLL
BMMC
PBMC
CD34+
C
ns
MDM2 basal Ct value
40
35
30
25
20
LC50< 1 μM
LC50> 1 μM
Sensitive responders
Intermediate/resistant
D
ns
PUMA basal Ct value
40
35
30
25
20
LC50< 1 μM
LC50> 1μM
Sensitive responders
Intermediate/resistant
E
MDM2 basal Ct value
40
35
30
25
20
r = 0.32
p = 0.12
0 1 2 3 4 5 6 7 8 9 10
RG7388 LC50 (μM)
F
PUMA basal Ct value
40
35
30
25
20
r = 0.26
p = 0.22
0 1 2 3 4 5 6 7 8 9 10
RG7388 LC50 (μM)

Figure S7

A

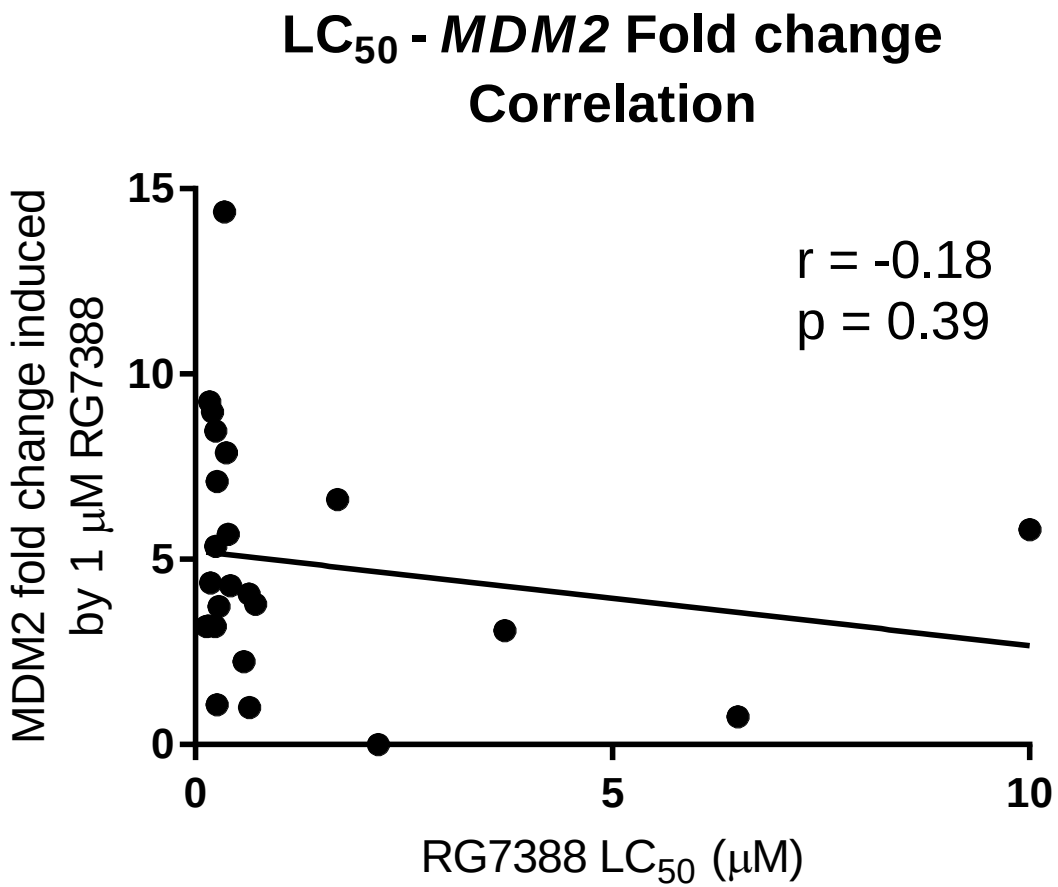
LC50 - MDM2 Fold change Correlation
MDM2 fold change induced by 1 μM RG7388
r = -0.18
p = 0.39
0
5
10
15
0
5
10
RG7388 LC50 (μM)

B

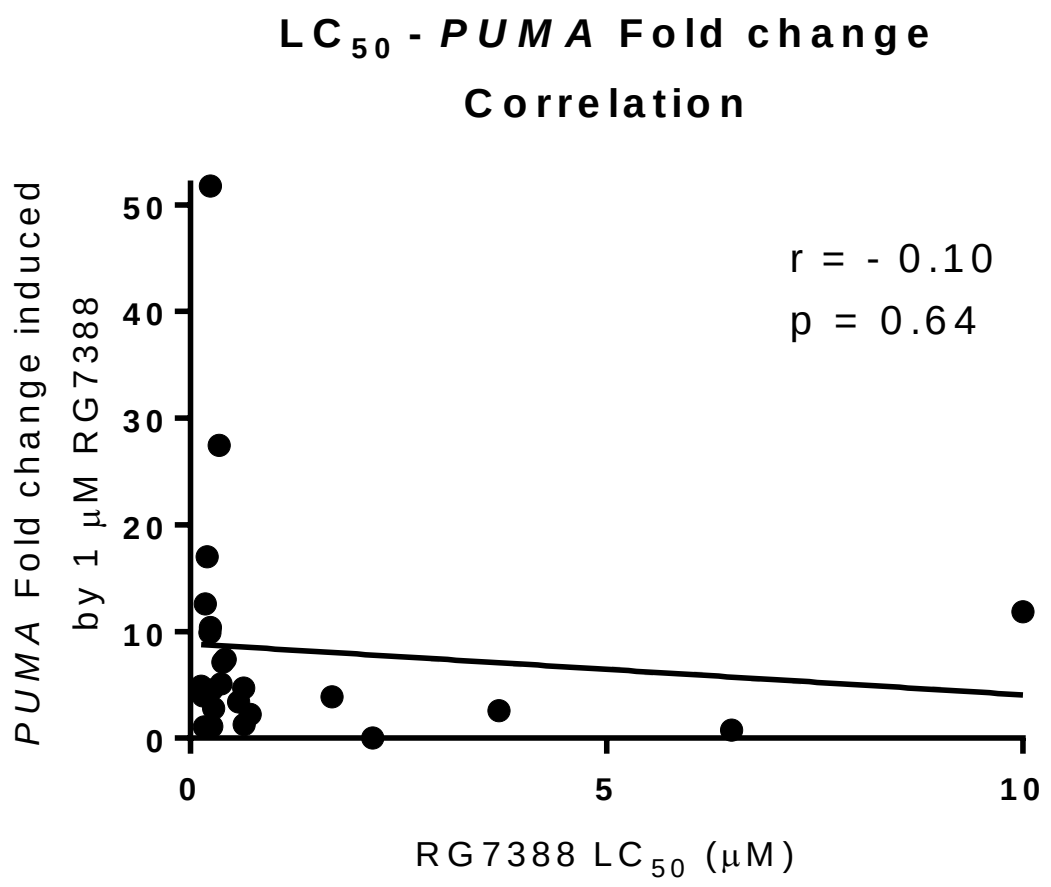
LC50 - PUMA Fold change Correlation
PUMA Fold change induced by 1 μM RG7388
r = - 0.10
p = 0.64
0
10
20
30
40
50
0
5
10
RG7388 LC50 (μM)

Figure S8

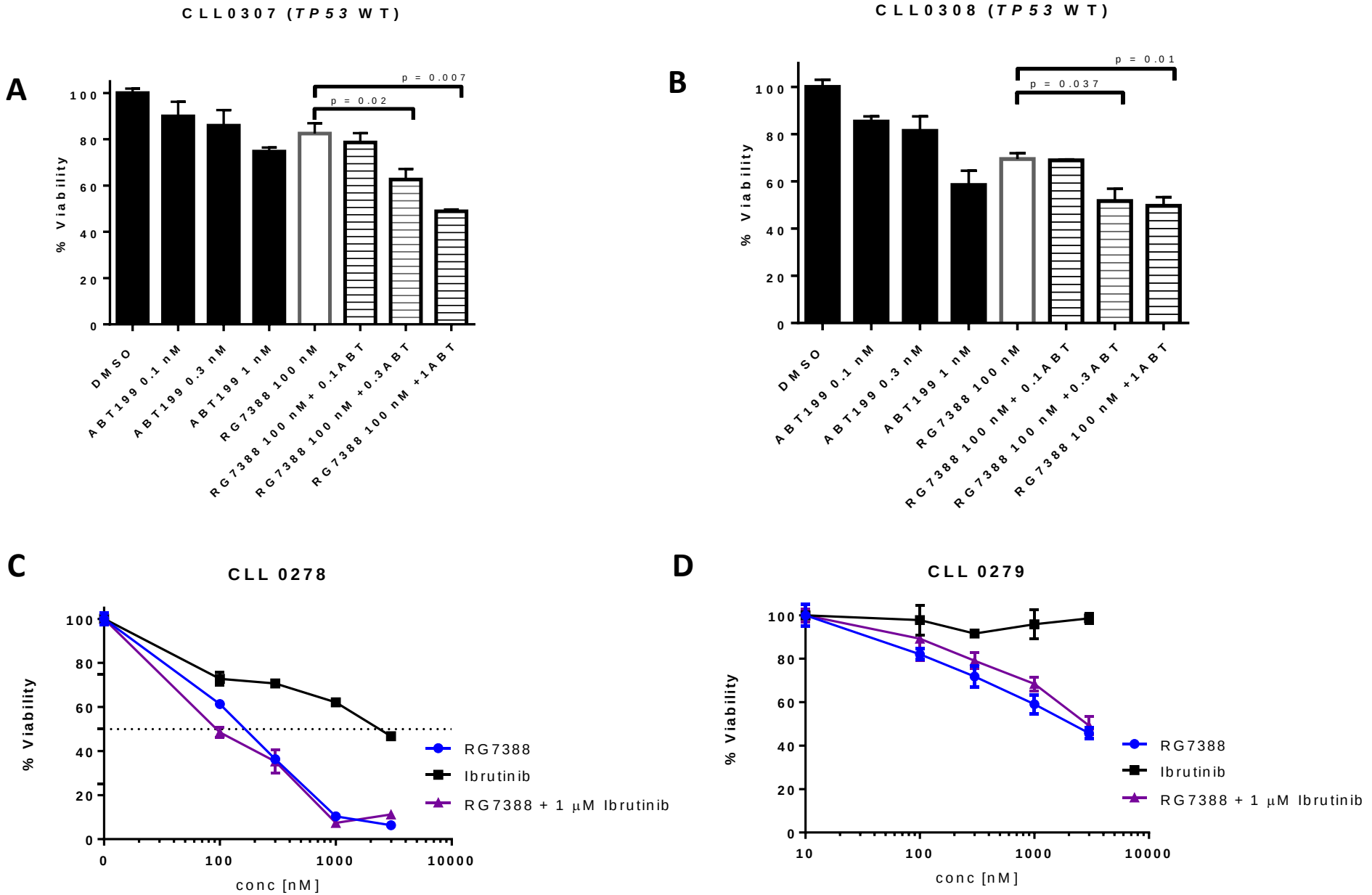
A
CLL0307 (TP53 WT)
% Viability
p = 0.007
p = 0.02
DMSO
ABT199 0.1 nM
ABT199 0.3 nM
ABT199 1 nM
RG7388 100 nM
RG7388 100 nM + 0.1ABT
RG7388 100 nM +0.3ABT
RG7388 100 nM +1ABT
B
CLL0308 (TP53 WT)
% Viability
p = 0.01
p = 0.037
DMSO
ABT199 0.1 nM
ABT199 0.3 nM
ABT199 1 nM
RG7388 100 nM
RG7388 100 nM + 0.1ABT
RG7388 100 nM +0.3ABT
RG7388 100 nM +1ABT
C
CLL 0278
% Viability
conc [nM]
RG7388
Ibrutinib
RG7388 + 1 μM Ibrutinib
D
CLL 0279
% Viability
conc [nM]
RG7388
Ibrutinib
RG7388 + 1 μM Ibrutinib